

**PREPRINT**

*Author-formatted, not peer-reviewed document posted on 19/01/2026*

DOI: <https://doi.org/10.3897/arphapreprints.e185559>

---

**Redescription of the osteology and systematic of  
*Panguraptor lufengensis* (Neotheropoda:  
Coelophysoidea)**

**Zechuan Zhang, Qixing Dong, Tao Wang, Hailu You, Xunlian Wang**

**For editors and reviewers: this is the finalized major revision from the first draft.**

**If there is any conflict in the content with the attached respond, this is the finalized content.**

**Redescription of the Osteology and Systematic of *Panguraptor lufengensis*  
(Neotheropoda: Coelophysoidea)**

Zechuan Zhang(1), Qixing Dong (2), Tao Wang(2), Hailu You(3), Xunlian Wang(1)

1. School of Earth Science and Resources, China University of Geosciences (Beijing), Beijing 100083, China
2. Center for Dinosaur Fossil Preservation and Research, Bureau of Land and Natural Resources of Lufeng City, Lufeng, Yunnan 650031
3. Key Laboratory of Vertebrate Evolution and Human Origins, Institute of Vertebrate Paleontology and Paleoanthropology, Chinese Academy of Sciences, Beijing 100044, China

**Abstract:** *Panguraptor lufengensis* You et al., 2014 is the first Coelophysoidea species that has been named in Asia. In previous studies, the description of holotype lacked anatomical details, leaving inadequate amounts of information. In this research, the anatomy is further described and the autapomorphic characters of *P. lufengensis* are re-evaluated, expanding into a combination of six characters. Phylogenetic analysis shows *P. lufengensis* is an early-branching member of the superfamily Coelophysoidea, indicating a yet to be uncovered ghost lineage of Coelophysoidea in East Asia.

**Key words:** Neotheropod, Coelophysoidea, Jurassic, Anatomy, Phylogeny

## 1. Introduction

### 1.1 A Brief Introduction of Coelophysoidea

Coelophysoidea was coined by Nopcsa in 1928, and the original definition of Coelophysoidea is the combination of all the “Triassic type” theropod dinosaurs. This definition has been revised multiple times. In Holtz (1994), the definition of Coelophysoidea was given as the most inclusive taxon formed by the descendants of the common ancestor of the Coelophysidae and *Dilophosaurus*, which forms the sister taxa of Neoceratosauria in the crown group Ceratosauria. This phylogenetic definition was re-tested in Sereno (2005), and the definition of Coelophysoidea was revised as the most inclusive clade including Coelophysis but not Carnotaurus, Ceratosaurus, and Passer. Neotheropod genera were once assigned within Coelophysoidea which are now most often recovered closer to Averostrans include *Dilophosaurus* (Welles, 1984; Tykoski 2005), *Zupaysaurus* (Ezcurra et al. 2007; You et al. 2014), *Liliensternus* (Rauhut and Hungerbühler 1998; Ezcurra and Cuny 2007), *Sarcosaurus* (von Huene 1932; Carrano and Sampson 2004; Ezcurra et al., 2023) and *Dracovenator* (Yates 2005). In conclusion, Coelophysoidea represents the first neotheropod clade that has a global contribution, offering significant paleogeographic and stratigraphic evidence for the evolution of non-avian dinosaurs.

Besides all the specimens that are named, there are specimens of Coelophysoidea that had been described but yet to be named from Lufeng, China (Irmis 2004), Skye Islands of Scotland (Kirmse et al., 2023), Tytherington fissure fills of England (Ezcurra et al. 2023), and Silesian Basin of Poland (Sulej et al. 2012; Qvanstrum et al. 2024).

## 1.2 The Brief Research History of Saurischian Fauna in Lufeng

The study of Lufeng Saurischian fauna (=Lufeng Dinosaurian fauna in Dong, 1982; Dong, 2001) started in 1938 with the discovery of one nearly complete skeleton of a sauropodomorph. Young studied it and named it *Lufengosaurus hueni* (Young, 1941). After the naming of *L. huenei*, the study of vertebrate fossils in Lufeng continues, and in 1951, Young named the whole fauna Lufeng Saurischian Fauna (Young, 1951). Besides dinosaurs, the Lufeng Saurischian Fauna is also famous for the rich records of mammaliaformes (Young, 1940; Young, 1947a; Chow and Hu, 1959; Patterson and Olsen, 1961; Chow, 1962; Rigney, 1963; Simmons, 1965; Cui, 1976; Young, 1978; Cui, 1981; Crompton and Sun, 1985; Luo and Sun, 1993; Crompton and Luo, 1993; Luo, 1994; Luo et al., 1994; Luo and Wu, 1995; Luo et al., 2001; Kielan-jaworowska et al., 2004; Averiano and Lopatin, 2014; Bi et al., 2014; Meng 2014; Mao et al., 2024; Hai et al., 2025), basal Archosaurs (Young, 1951; Simmons, 1965), crocodylomorphs (Young, 1944; Young, 1951; Simmons, 1965; Young, 1982; Wu and Sues, 1996; Harris et al., 2000; Wang et al., 2025) and lepidosaurs (Wu, 1994; Sues et al., 1994; Jones, 2006; Hsiou et al., 2015) are named and studied. This rich fossil record resembles one of the most diverse faunae during the Early Jurassic period.

In previous studies concerning Lufeng dinosaurian fauna, most studies is concerning the highly diversified sauropodomorph species, including genus *Lufengosaurus* (Young, 1941; Young, 1947b), *Yunnanosaurus* (Young, 1942; Lv et al., 2007), *Jingshanosaurus* (Zhang and Yang, 1985; Zhang et al., 2020), *Xixiposaurus* (Sekiya, 2010), *Xingxiulong* (Wang et al., 2018, Chen et al., 2025), *Yizhousaurus*

(Zhang et al., 2018) and *Lishulong* (Zhang et al., 2024). Compared to sauropodomorph, there are only three species of Neotheropod that have been studied and named, including *Sinosaurus triassicus* Young, 1948, *Lukousaurus yini* Young, 1948 and *P. lufengensis* You et al., 2014 (Xu et al., 2021). Beside three named species, in 2025, an incomplete specimen of new Averostra-line neotheropod is also reported (Li et al., 2025).

The fossils in Lufeng are found in two different layers of sediments. Most of the fossils, including the holotype of *P. lufengensis*, are discovered in the Shawan Members of Lower Lufeng Formation, identified as the dark red siltstone facies. Shawan Member lacks accurate dating since no volcanic activity is identified. Based on previous works concerning sequence stratigraphy and biostratigraphy (Sun, 1985; Ren et al., 2021), the age of Shawan Member is about 195 million years old.

Before the naming of *P. lufengensis*, in 1965, Simmons identified FMNH CUP-2089 and FMNH CUP-2090 as remnants of a member of genus *Podokesaurus*. Both specimens were part of the Catholic University of Peking Collection in Field Museum of Chicago, Illinois. According to Simmons, both specimens were collected in Lufeng County of Yunnan Province (Nowadays Lufeng city of Yunnan Province). In later works by Irmis (2004), both specimens were considered to belong to the same individual and reassigned them as remains of *Megapnosaurus*. In a long period of time, FMNH CUP2089 and FMNH CUP 2090 were the first certain fossil record of Coelophysoidea species in East Asia.

Following previous research, in 2008, a fossil research team assembled by Tao Wang discovered a complete skeleton with skull and mandible preserved in Dalishu

Village, Konglongshan Town of Lufeng County (nowadays Lufeng City). You et al. (2014) described the specimen and named it *Panguraptor lufengensis*. In the original works by You et al., 2014, the diagnosis of *P. lufengensis* is the combination of following three characters: 1) diagonal (=rostradorsal-caudoventral) ridge on lateral surface of maxilla, within antorbital fossa, 2) elliptical, laterally facing fenestra caudodorsal to aforementioned diagonal ridge, and 3) a hooked craniomedial corner of distal tarsal IV. In the same research, the position of *P. lufengensis* is recovered as a member within family Coelophysidae, with *Zupaysaurus* and *Liliensternus* recovered as the outgroups in the superfamily. In later research concerning other Coelophysoidea members, including *Lucianovenator bonoi*, *Powellvenator podocitus* and *Pendraig milnerae*, the position of *P. lufengensis* started swinging between the sister group of Coelophysidae (Martinez and Apaldetti 2017) and the sister group of genus *Syntarsus*. In the study concerning the evolution of body size among early neotheropods by Griffin (2019), the position of *P. lufengensis* is unstable and dropped in resolution.

**Abbreviations:** CUP – Catholic University of Peking Collection; FMNH - Field Museum of Chicago; LFGT/LFKL – Dinosaur Fossil Research and Reservation Center of Lufeng City.

## 2. Methods

In this research, we tested the phylogeny of *P. lufengensis* using the dataset originally published by Ezcurra et al., 2023, which is the latest update of Nesbitt et al., 2009 and its iteratively modifications, including Ezcurra and Brusatte, 2011; Sues et al., 2011; You et al., 2014; Nesbitt and Ezcurra, 2015; Martill et al., 2016; Ezcurra, 2017; Marínez and Apaldetti, 2017; Marsola et al., 2019a; Marsh et al., 2019; Griffin,

2019; Ezcurra et al., 2021a and Kirmse et al., 2023. The reason we choose the dataset from Ezcurra et al., 2023 is based on its degree of sampling within collection of members of Coelophysoidea. The data of *P. lufengensis* is modified based on the observation of the holotype in Mesquite 3.81. The matrix of this research includes 389 characters and 60 OTUs. The calculation of most parsimonious trees was done through New Technology tree branching processed on TNT version 1.6 (Goloboff et al. 2023), with *Erythrosuchus africanus* selected as the outgroup. As in Novas et al. 2021, the following characters were treated as additive: 9, 18, 30, 67, 128 – 129, 174, 184, 197, 207, 213, 219, 231, 236, 248, 253 – 254, 273, 329, 343, 345, 347, 349, 354, 366, 371, 374, 377 – 379, 383 – 384. Using the New Technology algorithm, a heuristic search of 1000 replications of Wagner trees with random addition sequence was performed, followed by TBR branch swapping holding 10 trees per replicate. Bremer (Bremer 1994), symmetric and bootstrap support values were calculated during resampling as using a ‘New Technology Search’ at 1000 iterations. Based on latest research concerning the stability of recovered evolutionary trees (Ezcurra 2024) to test for a more stable result by implying weight as equilibrium constant, the finalized result will be based on the recover result with implied weight  $K=12$ .

One important note is that the unnamed Coelophysoidea material introduced by Kirmse et al. 2023 would significantly reduce the resolution of recovered trees. Thus, in this research, we pruned the specimen reported in Kirmse et al., 2023 at the beginning.

### 3. Systematic Paleontology

Dinosauria Owen, 1842 sensu Langer et al. 2020

Theropoda Marsh, 1881 sensu Naish et al. 2020

Neotheropoda Bakker 1986 sensu Sereno 2005

Coelophysoidea Nopcsa 1928 sensu Sereno 2005

Genus *Panguraptor* You et al., 2014

**Type Species:** *Panguraptor lufengensis*

*Panguraptor lufengensis* You et al., 2014

**Holotype:** LFGT-0103, including a skeleton with skull and mandible. Based on interpretation in You et al. 2014 and a comparison with other Coelophysoidea specimens, the specimen belongs to a sub-adult individual.

**Occurrence:** The dark red sandstone facies of Shawan Member, Lower Lufeng Formation. One important note is that the specimen comes from the same sediments where famous *Lufengosaurus huenei* Young, 1941 was discovered. (Ren et al. 2021).

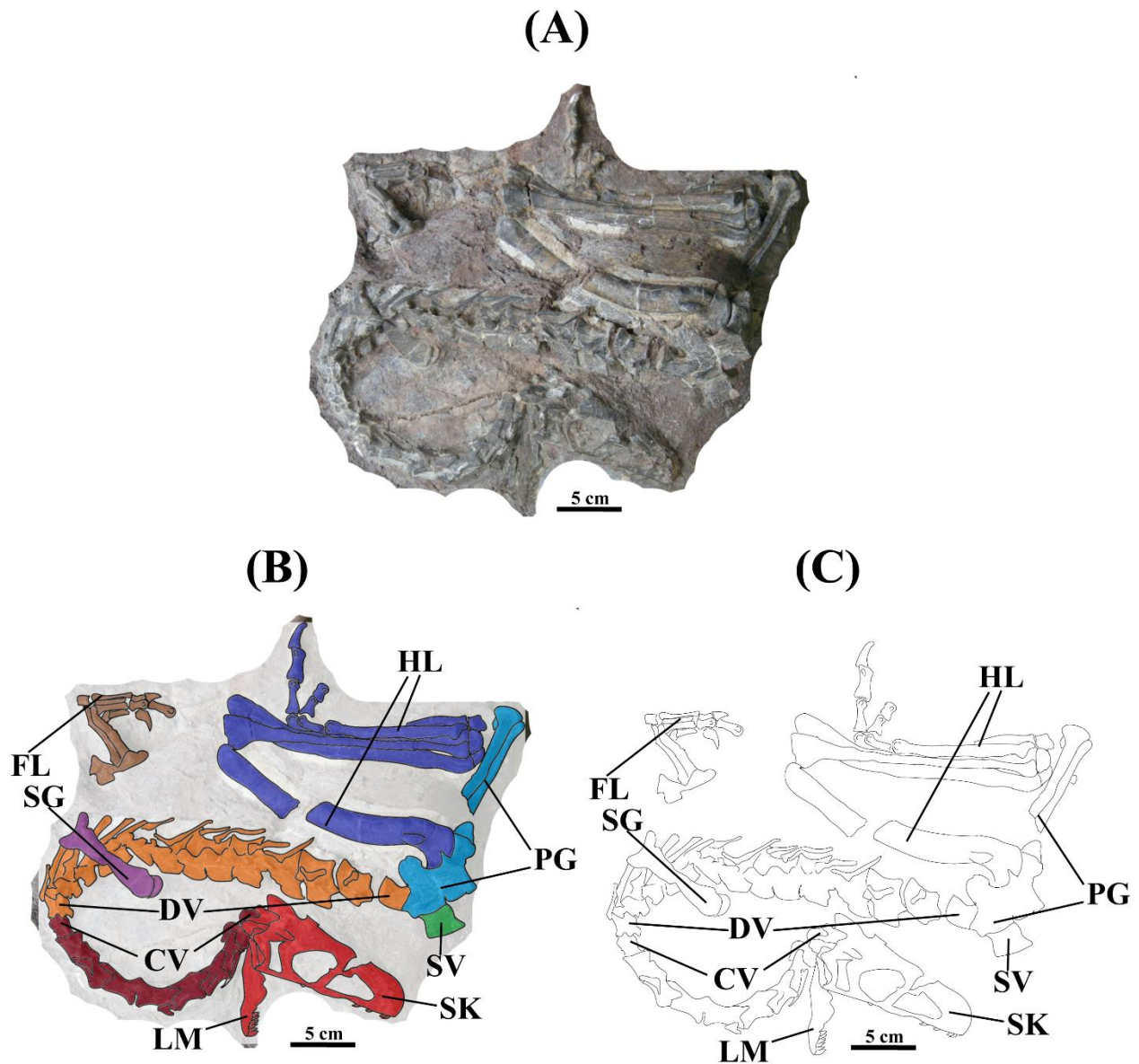


**Figure 3.1.** LFGT-0103 in lateral view, with the actual photo (A); the colored outline (B) and the sketch (C). Scale = 5 cm. Abbreviations: CV, cervical region; DV, dorsal region; FL, forelimb, HL, hindlimb, LM, mandibular region (=lower jaw); PG, pelvic gridle; SG, shoulder gridle; SK, skull; SV, sacral vertebrate.

**(For editors and reviewers, due to the settings of Microsoft Word 2025, this picture is compressed to fit in the page. This picture is edited in Adobe Illustrator and I do provide larger version. If you have reading problems, please find the attachment file for access of larger pictures.)**

**Diagnostic Characters:** Based on the observation in LFGT-0103, we revised the

diagnostic characters of *Pangraptor lufengensis*. The diagnostic character of *P. lufengensis* is the combination of following six characters (please note the asterisks indicate that the character is autapomorphic in *P. lufengensis*):

- (1) The diagonal (=rostradorsal-caudoventral) ridge over the lateral surface of maxillary diagonal to the ventral process. \* This was documented in You et al. 2014, however, it is observed here that the ridge elongated beyond the antorbital fossa and accompanied by a lateral shallow groove dorsal to it. Similar ridge is also documented in more derived species such as *S. triassicus* (Zhang et al. 2023) and other Averostr-line neotheropods, but in these species, the ridge is weakly developed.
- (2) A group of four elliptical, laterally facing fossae over the lateral surface of maxilla anterior to the antorbital fenestra, with one posterior to aforementioned diagonal ridge and three anterior to that ridge. \* This combination of small fenestrae observed in *P. lufengensis* is first-time recorded among neotheropods. This character was originally proposed by You et al. 2014.
- (3) The large, elliptic anterior pleurocoel over the lateral surface of cervical vertebrae from III to X. In other Coelophysoidea, the anterior pleurocoel in this region is sub-triangular. In Averostr-line species, such pleurocoel is sub-circular, such as what is observed in *D. wetherilli* (Marsh and Rowe, 2020).
- (4) The length of cervical rib equals to the anteroposterior length of centrum matching cervical vertebrae from cervical vertebrae III to VIII.\* In other

Coelophysoidea, the cervical ribs are elongated, as observed in *C. bauri* (Colbert, 1989), *M. rhodesiensis* (Raath 1977) and *Lucianovenator bonoi* (Martinez and Apaldetti, 2017).

(5) Distinct bony ridge over the dorsal margin on the lateral surface of scapula.

\* This is first-time recorded in neotheropod species and is considered autapomorphic to *P. lufengensis*. This character is also mentioned in You et al. (2014).

(6) The hook-shaped structure over the ventrolateral corner of proximal head of

distal carpal IV. \* This character is labeled in You et al. (2014) and is considered autapomorphic in *P. lufengensis* in this research as well.

## 4. Description

### 4.1 Skull and Mandible

The skull of LFGT-0103 is mostly complete. The anteroposterior length of the skull is 111 mm. The size of skull in LFGT-0103 is smaller than the adult of *Coelophysis bauri* (Colbert, 1989; Reinhart et al., 2009) and *Megapnosaurus rhodesiensis* (Raath, 1977), Averostra-line *Notatesseraeraptor frickensis* (Zahner and Brinkman, 2019), and close to *S. kayentakatae* (Rowe 1989; Tykoski 2002; Tykoski 2005), and significantly larger than the juvenile *C. bauri* (Bugos and McDavid 2024). Based on the observation in other Coelophysoidea specimens, the assumed ratio of length of antorbital fenestra versus length of skull in LFGT-0103 is much larger than *S. kayentakatae* (Rowe 1989; Tykoski 2005), immature *C. bauri* (Bugos and McDavid 2024), *Tawa hallae* (Nesbitt et al. 2009b), *Herrerasaurus ischigualastensis* (Serenio

and Novas 1994), and Averostra-line neotheropods including *N. frickensis* (Zahner and Brinkman 2019), genus *Sinosaurus* (Hu, 1993; Zhang et al. 2023), and *Dilophosaurus wetherilli* (Marsh and Rowe 2020), but close to mature individuals of *C. bauri* (Colbert 1989; Reinhart et al. 2009) and *M. rhodesiensis* (Raath 1977). The ratio between the dorsoventral height of antorbital fenestra in LFGT-0103 is close to average of members of Coelophysoidea including *C. bauri* (Colbert 1989; Reinhart et al. 2009) and *M. rhodesiensis* (Raath 1977), relatively smaller than *N. frickensis* (Zahner and Brinkman 2019), and significantly smaller than *Tawa hallae* (Ezcurra et al. 2009b), *H. ischigualastensis* (Sereno and Novas 1994), and Averostra-line members *Zupaysaurus rougieri* (Ezcurra 2006), genus *Sinosaurus* (Hu 1993; Zhang et al. 2023), and *D. wetherilli* (Marsh and Rowe 2020).

In LFGT-0103, the shape of orbit is subcircular, with a straight anterior border, this is similar to other species of Coelophysoidea (Raath 1977; Colbert 1989; Rowe 1989; Reinhart et al. 2009), but different from *T. hallae* (Ezcurra et al. 2009b), *H. ischigualastensis* (Sereno and Novas 1994) and Averostra-line members including *Z. rougieri* (Ezcurra 2006), genus *Sinosaurus* (Hu 1993; Zhang et al. 2023) and *D. wetherilli* (Marsh and Rowe 2020). In lateral view, the dorsal peak of skull is at the posterior part of the frontal instead of orbital level of the frontal. This is different from *T. hallae* (Ezcurra et al. 2009b) and *H. ischigualastensis* (Sereno and Novas 1994), and the juvenile *C. bauri* (Bugos and MaDavid 2024), but similar to the skull of mature *C. bauri* (Colbert 1989; Reinhart et al. 2009), *M. rhodesiensis* (Raath 1977) and '*S. kayentakatae* (Rowe 1989; Tykoski 2005), which the skull reaches the highest point over the dorsal region of frontal.

One important note concerning LFGT-0103 is that there are ossified elements within the anteroventral portion of the orbit. In this research, based on the location of these elements, we assumed the ossified elements could be preserved scleral ossicles. The boundary between each ossicle is not clearly visible due to poor preservation. The ossicles locate at the center of the orbit.

The mandible of LFGT-0103 is preserved, but the anterior and posterior tips are not visible. The teeth of holotype preserved in maxilla and dentary were severely damaged during the preparation, the remaining part of them are significantly smaller than other adult Coelophysoid specimens, including mature *C. bauri* (Colbert 1989; Reinhart et al. 2009; Buckley and Currie, 2014), *M. rhodesiensis* (Raath 1977) and *S. kayentakatae* (Rowe 1989; Tykoski 2005). In LFGT-0103, the mandible is mainly exposed from the right lateral side with only partial observation of left mandible from the medial side. The mandible of LFGT-0103 is mildly damaged from lateromedial side oppression. The length of measurable part of mandible is 111 mm, which will be applied for the estimation of total length of skull in this research.

In previous research by You et al. (2014), the presence of a well-marked external mandibular fenestra is labelled. Here we interpret the external mandibular fenestra in LFGT-0103 as being more elongated than previously suggested, and it located at a more posterior and dorsal position than what is described in You et al. (2014). A elongated external mandibular fenestra in the dorsal part of mandible is relatively common in early-derived dinosaurs and some neotheropods, including *T. hallae* (Ezcurra et al. 2009b), *H. ischigualastensis* (Sereno and Novas 1994), *N. frickensis* (Zahner and Brinkman 2019), but differs from the Coelophysoides *M. rhodesiensis*

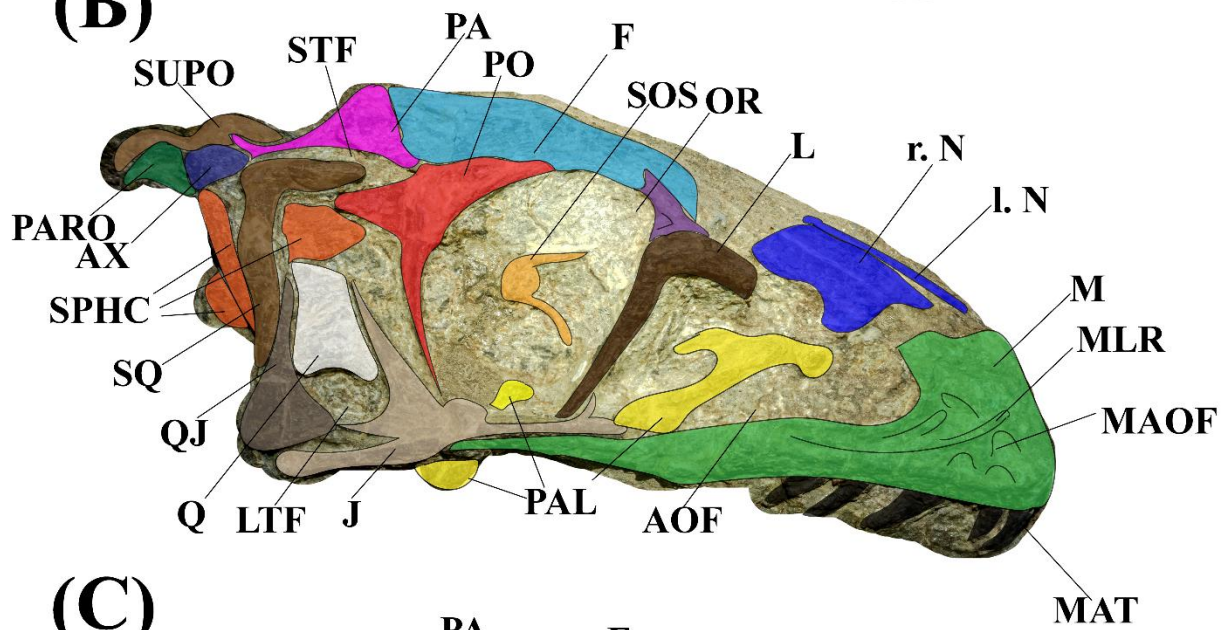
(Raath 1977) and *S. kayentakatae* (Rowe 1989; Tykoski 2005), and the stem-  
averostrans *Z. rougieri* (Ezcurra 2007), genus *Sinosaurus* (Hu 1993; Zhang et al.  
2023) and *D. wetherilli* (Marsh and Rowe 2020), which possess an external  
mandibular fenestra with much larger dorsoventral height and a much larger ratio  
between height and length. The presence of an external mandibular fenestra close to  
posterior part of mandible seen in LFGT-0103 is relatively common among  
neotheropods.

The length of alveolar line preserved on the dentary is 33 mm, and the ratio  
between the alveolar line and the total length of mandible is about 0.297. This ratio is  
significantly smaller than the average ratio of neotheropods.

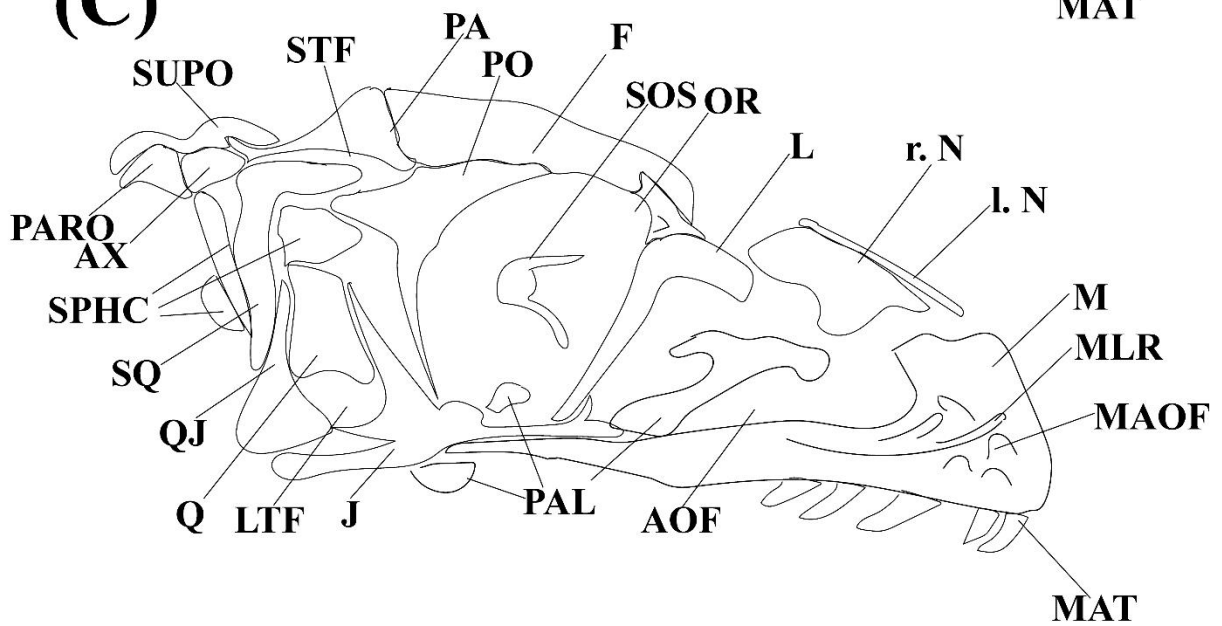
(A)



(B)



(C)



5 CM



**Figure 4.1.** The lateral view of the skull of LFGT-0103, including the original picture (A), the colored outline (B) and the sketch (C). Scale = 5 cm. Abbreviations: lowercase l. / r., left / right; AOF, antorbital fenestra; AX, axis; F, frontal;; J, jugal; L, lacrimal; LTF; lower temporal fenestra; M, maxilla; MAOF, maxillary antorbital fossae; MAT, maxillary teeth; MLR, maxillary lateral ridge; N, nasal; OR, orbit; PA, parietal; PARO, paroccipital process; PRF, pre-frontal; PAL, palatine; PO, postorbital; QJ, quadratojugal; SOS, scleral ossicle; SPHC, sphenoid complex; SQ, squamosal; STF, supratemporal fenestra; SUPO, supraoccipital

**(For editors and reviewers, due to the settings of Microsoft Word 2025, this picture is compressed to fit in the page. This picture is edited in Adobe Illustrator and I do provide larger version. If you have reading problems, please find the attachment file for access of larger pictures.)**

#### 4.1.1 Maxilla

Only the right maxilla is exposed from lateral view. The maxilla is composed of a ventral process and an ascending dorsal process. The maxilla is severely dislocated from its original position, with the posterior end of the ventral process reaches the posterior end of the skull from the ventral side of quadratojugal. Based on *C. bauri* (Colbert 1989; Reinhart et al. 2009) and *M. rhodesiensis* (Raath, 1977), the original location of maxillary ventral process should be joining the ventral ramus of the lacrimal and the anterior border of the jugal. The maxilla fenestra and the promaxillary foramen are not visible in the anterior portion of maxilla.

In the maxilla of *P. lufengensis*, one unique character is the distinct diagonal (=rostradorsal-caudoventral) ridge over the lateral side of the medial lamina, which

divides the lateral surface of maxilla ventral to the antorbital fenestra into two parts, the dorsal part that composes the ventral border of antorbital fenestra and the ventral part that participates on the external antorbital fenestra. In previous study by You et al. (2014), this was listed as one of three characters in the diagnostic characters combination. On contrary, based on the observations of other neotheropods, including Coelophysoids (Raath 1977; Colbert 1989; Rowe 1989; Tykoski 2005; Reinhart et al. 2009), Averostra-line neotheropods including *Sinosaurus* (Hu 1993; Zhang et al. 2023), *D. wetherilli* (Marsh and Rowe 2020) and averostrans such as *Allosaurus fragilis* (Madsen, 1976), *Ceratosaurus nasicornis*, the diagonal ridge in maxilla, which is interpreted as the pila interfenestralis, is a common pattern in many species. This ridge is absent in early-diverging dinosaurs such as *T. hallae* (Ezcurra et al. 2009b) and *H. ischigualastensis* (Sereno and Novas 1994) and species of Silesauridae. Thus, it is a reasonable conclusion that the diagonal or sub-parallel ridge is common among neotheropods, making it a possible apomorphic character to distinguish neotheropods from other dinosaurs. What is distinguish in LFGT-0103 is that the pila inter fenestralis is vertical, which is first-time record in all neotheropod species, making this character autapomorphic to *P. lufengensis*.

The posterior border of maxillary ascending process forms the anterior border of antorbital fenestra. The part of the process that contacts the lacrimal and frontal is lost, however, the remaining ascending process still occupies more than half of anterior border of both the external and internal antorbital fenestra. This is similar with members of Coelophysoidea (Raath 1977; Colbert 1989; Rowe 1989; Bugos and McDavid 2024), *Sinosaurus triassicus* and *Sinosaurus spp.* (Hu et al. 1993; Zhang et

al. 2023), *D. wetherilli* (Marsh and Rowe 2020), and *Z. rougieri* (Ezcurra 2007), which in all mentioned species, the posterior end of ascending process of maxilla constructs most of the antorbital fenestra. At the base of dorsal process, four foramina are visible over the lateral surface. Three of the four foramina located anterior to diagonal ridge described in last paragraph, and the one left is posterior to the diagonal ridge, anterior to the anterior angle of the internal antorbital fenestra. In previous research by You et al. (2014), the second character in the diagnostic characters combination is “the elliptical, laterally facing fenestra posterodorsal to the aforementioned diagonal ridge of maxilla.” In this research, this character is revised as follow – “the group of four elliptical, laterally facing foramina over the lateral surface of maxilla anterior to the antorbital fenestra, with one posterior to the aforementioned diagonal ridge of maxilla and three anterior to it.” The size of these foramina versus the size of antorbital fenestra in LFGT-0103 is larger than the average ratio of the size of promaxillary foramen versus antorbital fenestra in other neotheropods, and their position is different from promaxillary foramen in other neotheropods. However, it is highly possible that these foramina in *P. lufengensis* share same origin with the promaxillary foramen in other neotheropods. The large foramen at the base of ascending dorsal process in maxilla is not observed in Coelophysoids (Raath 1977; Colbert 1989; Rowe 1989; Reinhart et al. 2009; Bugos and McDavid 2024) nor in *N. frickensis* (Zahner and Brinkman 2019). In *H. ischigualastensis*, there is a foramen on the dorsal side of the dorsal process posterior to the external naris (Serenó and Novas 1994).

The preserved length of the maxillary ventral parallel process is 82 mm. From

lateral view, the ventral process of maxilla ends to the ventral side of the posterior end of antorbital fenestra. The length of the preserved maxilla occupies more than 70% of the existing skull. Taking the measure of the disarticulation of maxilla, the length of the antorbital fenestra would be larger than observed, and the maxillary alveolar line should be positioned in more anterior position. Among early dinosaurs and neotheropods, only some Coelophysoids (excluding *M. rhodesiensis* [Raath 1977]) and early-deriving saurischian *Eodromaeus murphi* (Martinez et al. 2011) possess a maxilla and maxillary alveolar line that extends to the ventral region of orbit, which is different from what is observed in LFGT-0103. The posterior end of maxilla is narrowed down into a tip. This is similar to other Coelophysidae species such as *C. bauri* (Colbert, 1989), *S. kayentakatae* (Rowe, 1989), and most Averostrine neotheropods such as *D. wetherilli* (Marsh and Rowe, 2020), *Sinosaurus triassicus* (Zhang et al., 2023), and Averostrine such as *Yuanmouraptor jinshajiangensis* (Zou et al., 2025) and *Asfaltovenator vialidadi* (Rauhut and Pol, 2019).

The preservation of maxillary teeth is poor. In observing the preserved maxillary teeth of LFGT-0103, the morphology and anatomy of maxillary teeth are same as the mandibular teeth, with the lingual end curving posteriorly, and serrations are presented on both sides down to the base.

#### **4.1.2 Nasal**

The nasal could only be observed from dorsal and right lateral view, and most of its element is lost. The preserved part of right nasal contacts the counterpart at the midline of skull, which is common among neotheropods.

#### **4.1.3 Lacrimal**

The lacrimal in LFGT-0103 is well-developed, sharing similar patterns with other Coelophysoidea species (Colbert, 1989; Reinhart et al., 2009, Raath, 1977; Rowe, 1989; Tykoski, 2005) and with the Averostra-line *N. frickensis* (Zahner and Brinkman 2019) and *S. triassicus* (Zhang et al. 2023).

The right lacrimal is exposed in lateral view, slightly displaced.. The lacrimal composes the dorsal margin of antorbital fenestra and the anterior margin of orbit. Due to disarticulation, the anterior process of lacrimal disarticulates from the nasal.

The length of the dorsal anterior process of the lacrimal is 17.4 mm, and the dorsoventral height of the ventral process is 28.5 mm. The dorsal body slightly convex dorsally, and its width maintains the same. This is same as what is observed in *C. bauri* (Colbert 1989; Reinhart et al. 2009; Bugos and McDavid 2024), but not only different from Coelophysoidea species *M. rhodesiensis* (Raath 1977) and *S. kayentakatae* (Rowe 1989; Tykoski 2005), and early-derived dinosaurs *E. murphi* (Martinez et al. 2011) and *H. ischigualastensis* (Serenó and Novas 1994), which the lacrimal blocked the prefrontal from participating the anterior border of orbit, but also different from *T. hallae* (Ezcurra et al. 2009b), which the ventral process of lacrimal bifurcates at the ventralmost tip.

Based on the observation, the ventral tip of lacrimal contacts the dorsal process of jugal . The ventral process of lacrimal shows differences from other Coelophysoidea members, and the ratio of anteroposterior length between the external naris (measuring from the anterior tip to the posterior tip) versus the external antorbital fenestra (measuring from the anterior tip to the posterior border at midpoint) and the ratio of anteroposterior length between the external antorbital fenestra versus the orbit

(measuring from the anterior border to the posterior border at the widest point) is close to *S. kayentakatae* (Rowe 1989; Reinhart 2009), whereas the anteroposterior length of external antorbital fenestra in *M. rhodesiensis* is much larger than other members of Coelophysoidea (Raath, 1977).

The ventral process of lacrimal narrowed from dorsal base towards the ventral tip, constructing a triangular-shaped structure from lateral view. With careful observation, there are small broken fractures over the anterior and anterodorsal border of ventral process, this indicates the possibility of a potential ossified fanlike structure that distinct the anterior portion from the posterior portion of prefrontal. The ventral process of lacrimal is similar to what is observed in *H. ischigualastensis* (Serenó and Novas 1994), *C. bauri* (Colbert 1989; Reinhart et al. 2009; Bugos and McDavid 2024), *M. rhodesiensis* (Raath 1977), *S. kayentakatae* (Rowe 1989; Tykoski 2005), *Dracoraptor hanigani* (Martill et al. 2016), and *S. triassicus* (Zhang et al. 2023), but different from *Z. rougieri* (Ezcurra 2006). The length of the ventral process measured from its ventral tip to dorsal base is larger than the anteroposterior length of the lacrimal. The posterior border of the ventral process composed most of the anterior border and small portion of dorsal border of orbit. The posterior process of the lacrimal is reduced and contacts the prefrontal.

#### 4.1.4 Prefrontal

The exposed right prefrontal includes the anterior and dorsal process which paralleled to the dorsal margin of orbit and a ventral process that narrowed down to the ventral tip. Comparing to Dinosauromorph such as *E. lunensis* (Serenó et al. 1993; Sereno et al. 2013) and early-deriving Saurischian such as *H. ischigualastensis*

(Sereno and Novas 1994), the prefrontal in LFGT-0103 is reduced in size and restricted to anterodorsal border of orbit, which appears to be the same with the short prefrontal observed in other Coelophysoidea species as well (Raath, 1977; Rowe, 1989). The main body of prefrontal is bar-shaped and occupies the anterodorsal corner of the orbit and mostly surrounded by frontal at medial and posterior border. This is similar in what is observed in other Coelophysidae members such as *C. bauri* (Colbert 1989; Reinhart et al., 2009), *S. kayentakatae* (Rowe 1989; Tykoski 2005) and *M. rhodesiensis* (Raath 1977). On contrary, as observed in averostrine neotheropod such as *D. wetherilli* (Marsh and Rowe, 2020) and *S. triassicus* (Zhang et al., 2023), the prefrontal occupies larger portion in the formation of antorbital fenestra.

There is a small depression over the lateral surface of prefrontal body in the anterior region, which represents the possibility that *P. lufengensis* might possess a pneumatic system over the lateral surface of prefrontal, which similar structure could be observed in the lateral surface of lacrimal and prefrontal of neotheropods such as Coelophysidae *C. bauri* (Reinhart et al., 2009) and *S. kayentakatae* (Rowe, 1989), Averostra-line *Z. rougieri* (Ezcurra 2007), *Sinosaurus spp.* (Hu 1993), *S. triassicus* (Zhang et al. 2023), *C. elloiti* (Smith et al. 2007), *D. wetherilli* (Marsh and Rowe 2020) and Averostra species, especially in Allosauridea such as *Yongchuanosaurus hepingensis* (Gao 1999) and *Allosaurus fragilis* (Madsen 1976).

#### 4.1.5 Scleral Ossicle

In You et al. (2014), the ossified structure at the center of orbit is not interpreted. In this research, after comparison, this bone structure is interpreted as the remaining of scleral ossicle. The scleral ossicle is mostly deformed and compressed, leaving limited

information concerning its development. The iridis in LFGT-0103 occupies much smaller portion than what is observed in *C. bauri* (Colbert 1989; Reinhart et al., 2009) and *S. kayentakatae* (Rowe 1989; Tykoski 2005).

#### 4.1.6 Postorbital

The postorbital is compressed at lateromedial direction slightly. From lateral view, the postorbital is composed of the descending ventral process that composes the posterior border of orbit and dorsal body at the posterodorsal side of the orbit. The postorbital does not develop an elongated and slime anterior process as observed in *Eoraptor lunensis* (Serenó et al. 1993; Sereno et al. 2013), *T. hallae* (Ezcurra et al. 2009b), *H. ischigualastensis* (Serenó and Novas 1994), Coelophysidae *C. bauri* (Colbert 1989; Reinhart et al. 2009), and averostrine *S. triassicus* (Zhang et al. 2023). The dorsal body of the postorbital participated in the formation of lateral border of supra-temporal fenestra from its medial border, which is similar to other members of Coelophysidae (Raath 1977; Colbert 1989; Rowe 1989; Tykoski 2005; Reinhart et al. 2009; Bugos and McDavid 2024). The ventral process is mediolaterally thin, articulated in its posterior margin with the posterior ascending process of jugal. The anterior border of the postorbital ventral process composes the entire posterior border of the orbit, and the lateral portion of its posterior process makes the anterodorsal border of the lower temporal fenestra. In lateral view, the surface of postorbital ventral process slightly concave, and the anterior border of the ventral process concave laterally. This ventral process contradicts to the convex posterior border of the dorsal process of jugal.

The anteroposterior length of the postorbital dorsal body is 24.9 mm, and the

height of ventral process is 28 mm with a ratio between the two portions of 0.89. The postorbital of LFGT-0103 is overall similar to adult *C. bauri* (Colbert 1989; Reinhart 2009), *S. kayentakatae* (Rowe 1989; Tykoski 2005), *N. frickensis* (Zahner and Brinkman 2019), *S. triassicus* (Zhang et al. 2023) and *D. wetherilli* (Marsh and Rowe 2020), but larger than immature *C. bauri* (Bugos and McDavid 2024). However, the short anterior process in LFGT-0103 is similar to what is observed in *S. kayentakatae* (Rowe 1989; Tykoski 2005).

#### 4.1.7 Frontal

The frontal exposed dorsolaterally. The anteroposterior length of the frontal is 54 mm. The lateral border of frontal makes up most of the dorsal margin of orbit, while the anterior margin articulates with the preorbital, the anteromedial margin contacts the nasal, the posterolateral margin articulates with postorbital, and the posteromedial margin contacts the parietal. On the dorsal side of the frontal, a sagittal ridge is developed, and it composes the highest tip of the skull. This is similar to adult *C. bauri* (Colbert 1989; Reinhart 2009) and *N. frickensis* (Zahner and Brinkman 2019). The ratio between the anteroposterior length of frontal versus the skull is between 0.33 to 0.5, which is close to *C. bauri* (Colbert 1989; Reinhart 2009) and Averostra-line theropods such as *S. triassicus* (Zhang et al., 2025) and Averostra such as *A. vialidadi* (Rauhut and Pol, 2019), slight larger than *E. lunensis* (Serenó et al. 1993; Sereno et al. 2013), *T. hallae* (Ezcurra et al. 2009b) and *H. ischigualastensis* (Serenó and Novas 1994).

On the posteromedial side of the frontal, which is the region that frontal articulates with the parietal, a distinct subtriangular depression is formed. This

depression is the fossa of supratemporal fenestra, which is also documented on *C. bauri* (Colbert 1989; Reinhart 2009), *S. kayentakatae* (Rowe 1989, Tykoski 2005) and *N. frickensis* (Zahner and Brinkman 2019). As found in other early-diverging dinosaurs and Coelophysoids species, in LFGT-0103, the frontal does not participate in the formation of supratemporal fenestra. The lateral margin of frontal forms a convex margin over the dorsal margin of orbit, which extends to the prefrontal and postorbital. In *S. kayentakatae*, the frontal forms a lateral crest in this region (Rowe 1989; Tykoski 2005), and in *M. rhodesiensis* (Raath, 1977) and *C. bauri* (Colbert 1989; Reinhart et al. 2009; Bugos and McDavid 2024), the dorsal margin of the orbit is smooth.

#### 4.1.8 Parietal

The parietal exposed from lateral and posterior view. In the lateral view, a depression is visible between continuity from the peak of frontal sagittal ridge to the peak of the parietal sagittal ridge. In modern birds and crocodylians, this sagittal crest supports the occlusal muscles through the supratemporal fenestra and the lower temporal fenestra. This strongly developed sagittal ridge in *P. lufengensis* is first-time record in Coelophysidae such as *C. bauri* (Colbert, 1989) and *M. rhodesiensis* (Raath, 1977), in which the dorsal surface of parietal is flat or slightly convex., .

From posterior and dorsal view, the supratemporal fenestra is subtriangular, with its medial tip located at the lateral border of parietal. From lateral view, the parietal develops a ridge at its peak, which forms the dorsal tip of sagittal ridge, and composed the dorsal tip of supratemporal fenestra from lateral side.

#### 4.1.9 Jugal

Not originally labelled in You et al. 2014, the anterior tip of the jugal participates in the dorsoventral corner of the antorbital fenestra, and there is a weakly developed anterior ascending dorsal process visible laterally, which is supposed to contact the ventral process of lacrimal from its medial side. This indicates that the lacrimal and jugal articulate with each other. Among other Coelophysoidea species, the jugal is barred from antorbital fenestra by lacrimal, such as *C. bauri* (Colbert 1989; Reinhart et al. 2009), *S. kayentakatae* (Rowe 1989; Tykoski 2005), and *M. rhodesiensis* (Raath 1977). In contrary, this character is common among other dinosaurs, such as *E. murphi* (Martinez et al. 2011), *H. ischigualastensis* (Sereno and Novas 1994), *T. hallae* (Nesbitt et al. 2009b), *E. lunensis* (Sereno et al. 1993; Sereno et al. 2013), and Averostra-line neotheropods such as *N. frickensis* (Zahner and Brinkman 2019), *D. wetherilli* (Marsh and Rowe 2020), *Z. rougieri* (Ezcurra 2007), *Sinosaurus triassicus* (Zhang et al. 2023) and *Cryolophosaurus ellioti* (Smith et al. 2007).

The main body of jugal is overlapped by disarticulated maxilla, but the part that composed the ventral border of orbit is visible. The posterior ascending dorsal process is distinct, with a height of 22.1 mm measured from the ventral bottom to dorsal tip, only slightly shorter than the postorbital descending ventral process. In You et al. (2014), the parallel posterior process is bifurcated, and in this research, it is observed and indicated that the jugal is not bifurcated in this region, which is similar to other Coelophysoidea species, but different from other neotheropods, including *H. ischigualastensis* (Sereno and Novas 1994), *E. murphi* (Martinez et al. 2011), and early Averostra-line members, including *D. wetherilli* (Marsh and Rowe 2020), *Z. rougieri* (Ezcurra 2006), *Sinosaurus triassicus* (Zhang et al. 2023) and

*Cryolophosaurus ellioti* (Smith et al. 2007).

#### 4.1.10 Quadratojugal

The quadratojugal is exposed in right lateral view. The quadratojugal contacts squamosal from the posterior side of dorsal ascending process in its dorsal portion. In the specimen, the quadratojugal articulated with jugal from the ventral side of the ventral process to the dorsal side of posterior end of jugal. The anterior process of quadratojugal in LFGT-0103 is not elongated, only within the posterior border of lower temporal fenestra, this is different from *H. ischigualastensis* (Sereno and Novas 1994) and *E. murphi* (Martinez et al. 2011), and early Averostra-line taxa, including *D. wetherilli* (Marsh and Rowe 2020), *Z. rougieri* (Ezcurra 2006), *Sinosaurus triassicus* (Zhang et al. 2023) and *Cryolophosaurus ellioti* (Smith et al. 2007), which the quadratojugal possessed an elongated anterior process that construct the ventral border of lower temporal fenestra. However, it is similar with the quadratojugal in *C. bauri* (Colbert 1989; Reinhart et al. 2009) and *M. rhodesiensis* (Raath 1977).

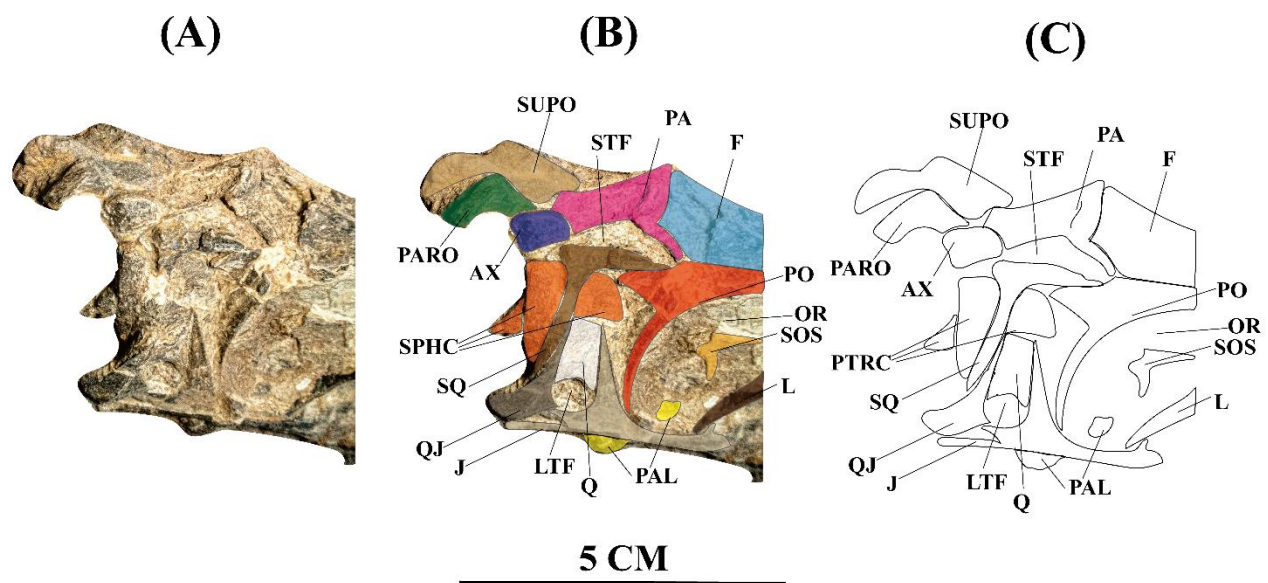


**Figure 4.2.** The posterolateral view of posterior portion of the skull of LFGT-0103

including the original picture (A), the colored outline (B) and the sketch (C). Scale = 5 cm. Abbreviations: AX, axis; F, frontal;; J, jugal; L, lacrimal; LTF; lower temporal fenestra; N, nasal; OR, orbit; PA, parietal; PARO, paroccipital process; PAL, palatine; PO, postorbital; QJ, quadratojugal; SOS, Scleral Ossicle; SPHC, sphenoid complex; SQ, squamosal; STF, supratemporal fenestra; SUPO, supraoccipital

**(For editors and reviewers, due to the settings of Microsoft Word 2025, this picture is compressed to fit in the page. This picture is edited in Adobe Illustrator and I do provide larger version. If you have reading problems, please find the attachment file for access of larger pictures.)**

#### **4.1.11 Quadrate**

The quadrate is only exposed in right lateral view. In this view, the dorsal head of the quadrate is subcircular, the rest of the quadrate dorsal process share the equal width of the dorsal head. This character is different from other neotheropods, as the more generalized character is that the width of quadrate is gradually narrowed down towards the dorsal head. However, it is impossible to rule out the possibility of deformation during fossilization is the cause behind this phenomenon in LFGT-0103.

Most of the lateral body of quadrate is board, making it fill most of the lower temporal fenestra. In lateral view, theexposed part of quadrate in LFGT-0103 is much larger than what is observed in early theropods such as *H. ischigualastensis* (Serenio and Novas, 1994), *T. hallae* (Nesbitt et al., 2009), other Coelophysidae members such as *C. bauri* (Colbert, 1989; Reinhart et al., 2009).

#### **4.1.12 Squamosal**

The squamosal, visible from lateral view and dorsal view, is composed of the

anterior process on the dorsal side of the skull and the ventral process narrowed towards the ventral end. The anterior process of squamosal participated in the lateral border of supratemporal fenestra and the dorsal border of lower temporal fenestra, while the ventral process participated in the posterior border of lower temporal fenestra. The ventral process contacts the ascending process of quadratojugal from its posterior side, which is similar to *C. bauri* (Colbert 1989; Reinhart et al. 2009) and *S. kayentakatae* (Rowe 1989; Tykoski 2005), but different from *M. rhodesiensis*, the species that squamosal developed a short ventral process (Raath 1977). The angle between the anterior process and the ventral process is about 80 degrees, which is larger than what is measured in specimens of *C. bauri* (Colbert 1989; Reinhart et al. 2009) and *S. kayentakatae* (Rowe 1989; Tykoski 2005), but similar to averostran-line neotheropods, including *N. frickensis* (Zahner and Brinkman 2019), *D. wetherilli* (Marsh and Rowe 2020), *Z. rougieri* (Ezcurra 2006), *Sinosaurus triassicus* (Zhang et al. 2023) and *Cryolophosaurus ellioti* (Smith et al. 2007). In lateral view, the squamosal in LFGT-0103 is similar to other Coelophysoidea except *M. rhodesiensis* (Raath 1977), however, the ratio of the length of ventral process versus the length of the anterior process of LFGT-0103 is much larger than other Coelophysoidea species except *S. kayentakatae* (Rowe 1989; Tykoski 2005).

#### 4.1.13 Palatine

The palatine is visible in lateral view, showing both the anterior portion within antorbital fenestra and the posterior end ventral to orbit. The anterior portion in antorbital fenestra is not fully preserved, but the remaining part still occupies more than 50% of the antorbital fenestra, with the dorsoventral height of palatine occupies

more than 50% of the antorbital fenestra. This ratio is similar to other Coelophysoidea members (Colbert, 1989; Rowe, 1989), as they have large vomers as well, but it is still larger than other species. However, since the skull is severely deformed, the actual portion of palatine could be smaller. In *C. bauri*, the posterior end of palatine stops anterior to the orbit (Colbert, 1989). The round palatine posterior head in LFGT-0103 matches what is observed in *M. rhodesiensis* (Raath, 1977; Colbert, 1989).

#### **4.1.14 Supraoccipital**

The supraoccipital is exposed dorsally. From the exposed part, the lateral surface of supraoccipital is flat and smooth. The posterior part is disoriented by the pressure of paroccipital process.

#### **4.1.15 Paroccipital process**

The paroccipital process is preserved and could be viewed laterally. In lateral view, the paroccipital process is flat in dissection shape. Since it's not fully exposed, the total length of the paroccipital is not available. Comparing to Coelophysidae members such as *C. bauri* (Colbert, 1988), *M. rhodesiensis* (Raath, 1977), and *S. kayentakatae* (Rowe, 1989; Tykoski, 2005), the paroccipital process in LFGT-0103 is similar in shape and size, which is also observed in the paroccipital process of Averostra-line neotheropods, such as *D. wetherilli* (Marsh and Rowe 2020), *D. hanigani* (Martill et al. 2016), and *S. triassicus* (Zhang et al., 2023).

#### **4.1.16 Sphenoid complex**

In this research, with careful examination, the basisphenoid is observed from lateral view. The basisphenoid is exposed in lateral view within lower temporal fenestra. However, there are no observable characters preserved in this element due to

the state of preservation.

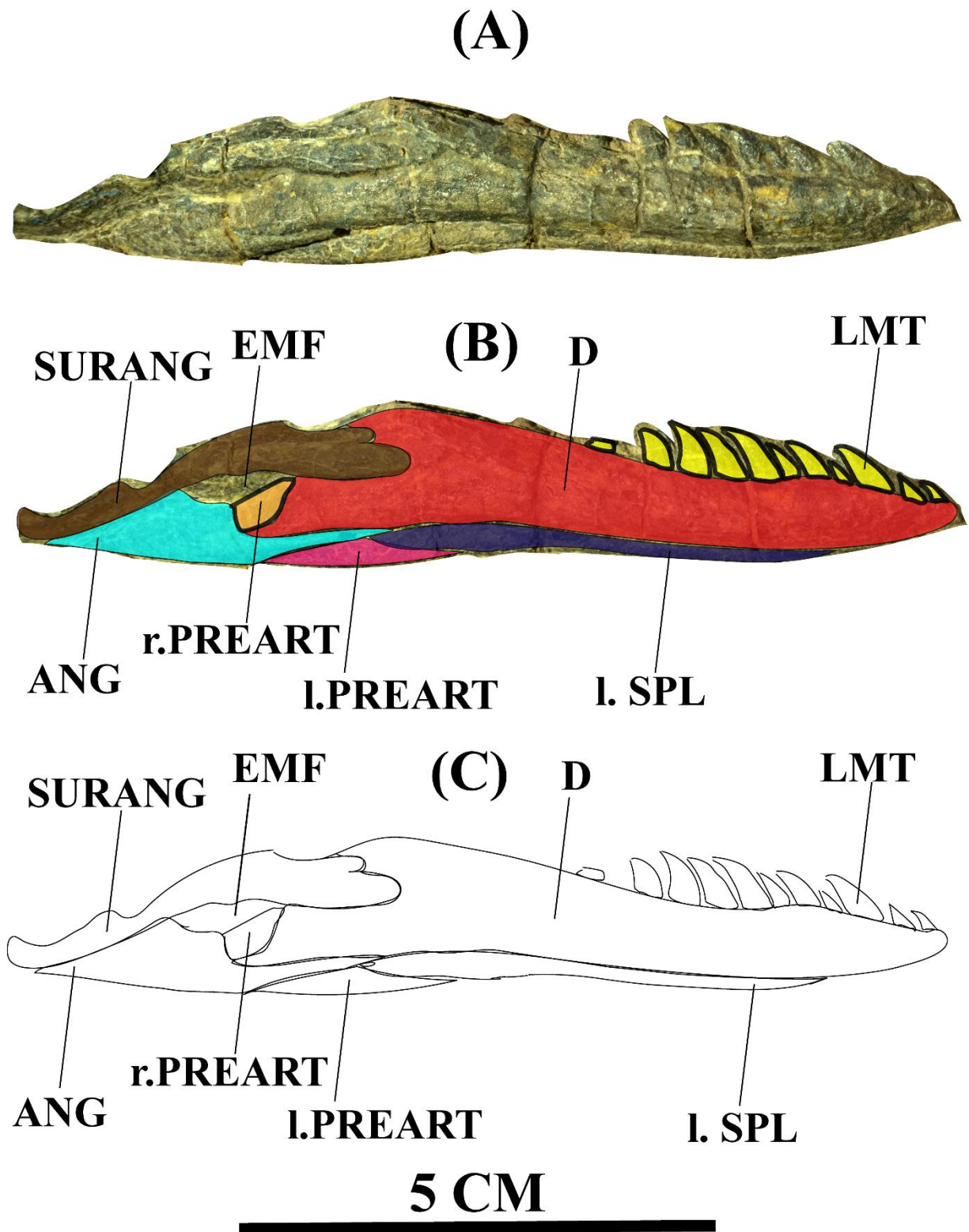


**Figure 4.3.** The exposed portion of mandible in lateral view and the matching outline.

Scale = 5 cm. Abbreviations: lowercase l. / r., left / right; ANG, angular; D; dentary;

EMF, external mandibular fenestra; PREART, left prearticular; SPL, left splenial;  
LMT, dentary teeth; SURANG, surangular.

**(For editors and reviewers, due to the settings of Microsoft Word 2025, this picture is compressed to fit in the page. This picture is edited in Adobe Illustrator and I do provide larger version. If you have reading problems, please find the attachment file for access of larger pictures.)**

#### 4.1.17 Dentary

The suture between the dentary, the angular and the surangular is unclear in LFGT-0103. The dentary groove is not visible over the lateral surface of anterior portion of dentary. The width of the maxilla remains basically the same until the second last preserved dentary tooth. In LFGT-0103, the alveolar line starts expanding dorsally posterior to the second dentary tooth and end at the last dentary tooth, while the ventral border of dentary becomes concaved, which is more abrupt than other neotheropods, including *T. hallae* (Ezcurra et al. 2009b), *H. ischigualastensis* (Serenó and Novas 1994), *E. murphi* (Martinez et al. 2011), Coelophysoidea, *N. frickensis* (Zahner and Brinkman 2019), *D. wetherilli* (Marsh and Rowe 2020), but similar to *E. lunensis* (Serenó et al. 1993; Sereno et al. 2013).

Starting at the anterior portion of the dentary, a groove is visible over the lateral surface of the mandible, which extends to the posterior portion of it. The groove is divided by the external mandibular fenestra, then extends separately over the lateral surface of angular and surangular. This groove does not develop gradually but appears suddenly at the midline of the surface.

There are 11 teeth preserved in dentary, the ratio between the length of preserved

mandibular teeth role to measurable lower mandibular is 0.396, and the ratio between the length of mandibular teeth role to maxillary teeth role is 0.53, which is close to other Coelophysoidea species, but smaller than other neotheropods.

#### **4.1.18 Angular**

In LFGT-0103, the angular is severely disformed as most of the posterior part of mandible is severely disformed and compressed. The angular articulates with the posterior portion of the ventral margin of the dentary end of dentary from its anterior end, forming the ventral margin of the external mandibular fenestra. The angular forms the posterior portion of the ventral border of external mandibular fenestra.

#### **4.1.19 Surangular**

In LFGT-0103, the surangular composes the dorsal region of the external mandibular fenestra. The dorsal side of the surangular possesses the continuous ossified ridge extended from the dorsal side of dentary. At the posterior tip of mandible, the surangular enlarged.

One unique character in LFGT-0103 is that the anterior dorsal process of surangular formed the second highest point of whole mandible, and a concavity formed between this peak and the anterior peak on dentary. This is rare in neotheropods, as this is absent in other Coelophysoidea species (Raath, 1977; Colbert, 1989; Rowe, 1989), *Averostra-line D. wetherilli* (Marsh and Rowe, 2020), *S. triassicus* (Zhang et al., 2023) and *Averostra* such as *Y. jinshajiangensis* (Zou et al., 2025), *A. vialidadi* (Rauhut and Pol, 2019) .

#### **4.1.20 Splenial Bone**

In LFGT-0103, the left splenial bone over the medial side of the left mandible is

exposed at its ventral end. From the exposure, the splenial bone is thin, which is the common pattern among archosaurs.

#### 4.1.21 Prearticular

In LFGT-0103, part of the prearticular is visible, constructing the internal mandibular fenestra. The dorsal border of preserving prearticular is straight.

#### 4.2 Vertebrae and Ribs

In LFGT-0103, the specimen preserved a sequence of vertebrae, consisting of 12 cervical vertebrae, 13 dorsal vertebrae and the first sacral vertebra. Most of the cervical and dorsal ribs are broken and lost their distal end, so it's impossible to determine their length.

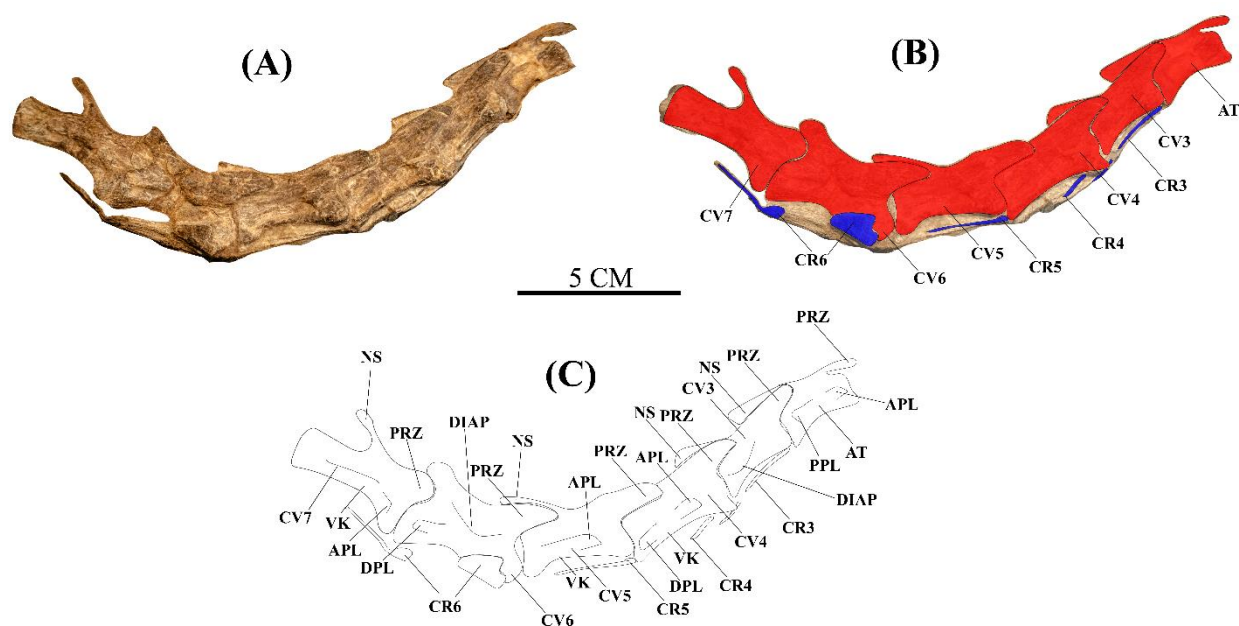


**Figure 4.4.** The anterior and middle portion of cervical vertebrae column of *Panguraotor lufengensis* in lateral view, showing the column from the atlas to cervical vertebra 7 (CV7), including the picture (A), the colored outline (B) and the sketch (C). Scale = 5 cm. Abbreviations: AT, atlas; APL, anterior pleurocoel; CR, cervical rib; CV, cervical vertebrae; DIAP, diapophyses; NS, neural spine; PPL, posterior

pleurocoel; PRZ, prezygapophysis. VK, ventral keel.

**(For editors and reviewers, due to the settings of Microsoft Word 2025, this picture is compressed to fit in the page. This picture is edited in Adobe Illustrator and I do provide larger version. If you have reading problems, please find the attachment file for access of larger pictures.)**

#### 4.2.1 Cervical Vertebrae

Due to the loss of abdominal ribs, we consider the last cervical vertebra to be the last vertebra that does not contact scapula anterior to scapula, which calculates up to 10 cervical vertebrae including atlas and axis. This number matches what is observed in *C. bauri* (Colbert 1989; Reihart et al. 2009) and *L. bonoi* (and Apaldetti Martinez 2017), but smaller than what is observed in averostr-line dinosaurs such as *S. sinensis* (Hu 1993). The total length of cervical vertebrae is 250 mm. The total length of the skeleton and the femur of LFGT-0103 is unknown so it is not possible to determine the development of cervical region in relation to the whole body.

Coelophysoidea. In LFGT-0103, the atlas and axis are preserved in bad condition. The atlas is only exposed partially from the lateral side. One thing that is certain is that the width of the atlas is similar to the width of the axial centrum anterior surface.

You et al. (2014), gave the anteroposterior length of the axis as 18.5 mm, which we reaffirm. The neural spine of axis is incomplete, and the centrum is exposed from anterior and lateral view. The prezygapophysis is broken and missing, leaving a circular dissection over the anterodorsal surface of axis.

Posterior to the axis, all eight cervical vertebrae in LFGT-0103 specimen are preserved but only exposed in right lateral view. There are gaps between cervical

vertebrae VI, VII, VIII and IX, clear broken edges presented over the cervical vertebrae VII and VIII, and the centrum anterior surface of cervical vertebrae IX. Provided in earlier study by You et al. (2014), the anteroposterior length of centrum of cervical vertebrae from cervical vertebrate III to X is 24 mm, 28 mm, 29 mm, 31 mm, 30.5 mm, 28.5 mm, 28 mm and 23 mm. Comparing this data to *L. bonoi* (Martinez and Apaldetti 2017) and adult *C. bauri* (Reinhart et al. 2009), the cervical vertebrae of same position is on average 10% to 20% smaller in *P. lufengensis*.

In LFGT-0103, the cervical vertebrae at the middle of the column are elongated. Taking cervical vertebrate IV as an example, the ratio between the anteroposterior length of centrum and the height of posterior articular surface of centrum is about 2.77, and the ratio between the anteroposterior length and the total height of the vertebrate including the neural arch is 1.45. This phenomenon is relatively common among early small neotheropods, including *Liliensternus liliensterni* (Ezcurra and Cuny 2007), *C. bauri* (Colbert 1989; Reinhart 2009), and *L. bonoi* (Martinez and Apaldetti 2017)..

In lateral view, in *P. lufengensis*, , the margin of anterior and posterior centrum articular surface of cervical vertebra III to VI is nearly straight, and it is observed in at least cervical vertebrate V and VI that the centrum surface is depressed, which is same with other neotheropods including both Coelophysoidea and averostr-line, but different from early-derived species, including *H. ischigualastensis* (Sereno and Novas 1994), *Sanjuansaurus gordilloi* (Alcober and Martinez 2010) and *E. murphi* (Martinez et al. 2011).

*Panguraptor* retains pronounced pleurocoels structure in the postaxial cervical

vertebrae with the most pronounced ones in vertebra VII. There are two pairs of pleurocoels over the lateral surface of the cervical vertebrae, the anterior pleurocoel of the centrum shapes as a nearly triangular fossa, which possesses relatively straight dorsal and anterior margins. The posterior pleurocoel is located on the posterior centrum at a level anterior to the postzygapophysis and is shallow in its centre. The anterior pleurocoel of cervical vertebrae demonstrates different structure from *C. bauri* (Colbert 1989), *M. rhodesiensis* (Raath 1977), *S. kayentakatae* (Rowe 1989), and *L. bonoi* (Martinez and Apaldetti 2017) since these species preserved elliptical pleurocoel. There is no evidence of a small pleurocoel at the centrodiaepophyseal lamina as observed in *L. bonoi* (Martinez and Apaldetti 2017). The presence of a ventral keel is observed in cervical vertebrae from III to X, which is also observed in *L. bonoi* (Martinez and Apaldetti 2017), *C. bauri* (Colbert 1989) and *M. rhodesiensis* (Raath 1977). The depth of anterior and dorsal surface of centrum in cervical vertebrae does not vary significantly, which is similar to *C. bauri* (Colbert 1989).

In *Panguraptor lufengensis*, the neural arches of the postaxial cervical vertebrae are ossified to the centrum. The ventrolateral articular facet of prezygapophysis articulates with postzygapophysis of previous vertebrae from its dorsomedial side. No clear depression or fossa is present over the lateral surface of prezygapophysis and postzygapophysis of cervical vertebrae. The preserved neural spine of cervical vertebrae does not strongly develop in LFGT-0103, forms a sagittal-shape fan on the dorsal side of the vertebrae. The diapophysis of cervical vertebrae is elongated anteroventrally, which is similar to other Coelophysoids (Raath, 1977; Colbert 1989; Rowe 1989; Martinez and Apaldetti 2017). Starting from the cervical vertebrae VIII

posteriorly, the length of centrum shortens. The anteroposterior length of cervical vertebrate X is close to cervical vertebrate III. This shortening is common among Coelophysoidea (Raath, 1977; Rowe, 1989; Marrinez and Apaldetti, 2017). Unlike dorsal vertebrae, in the cervical vertebrae of LFGT-0103, the diapophysis does project straight laterally.

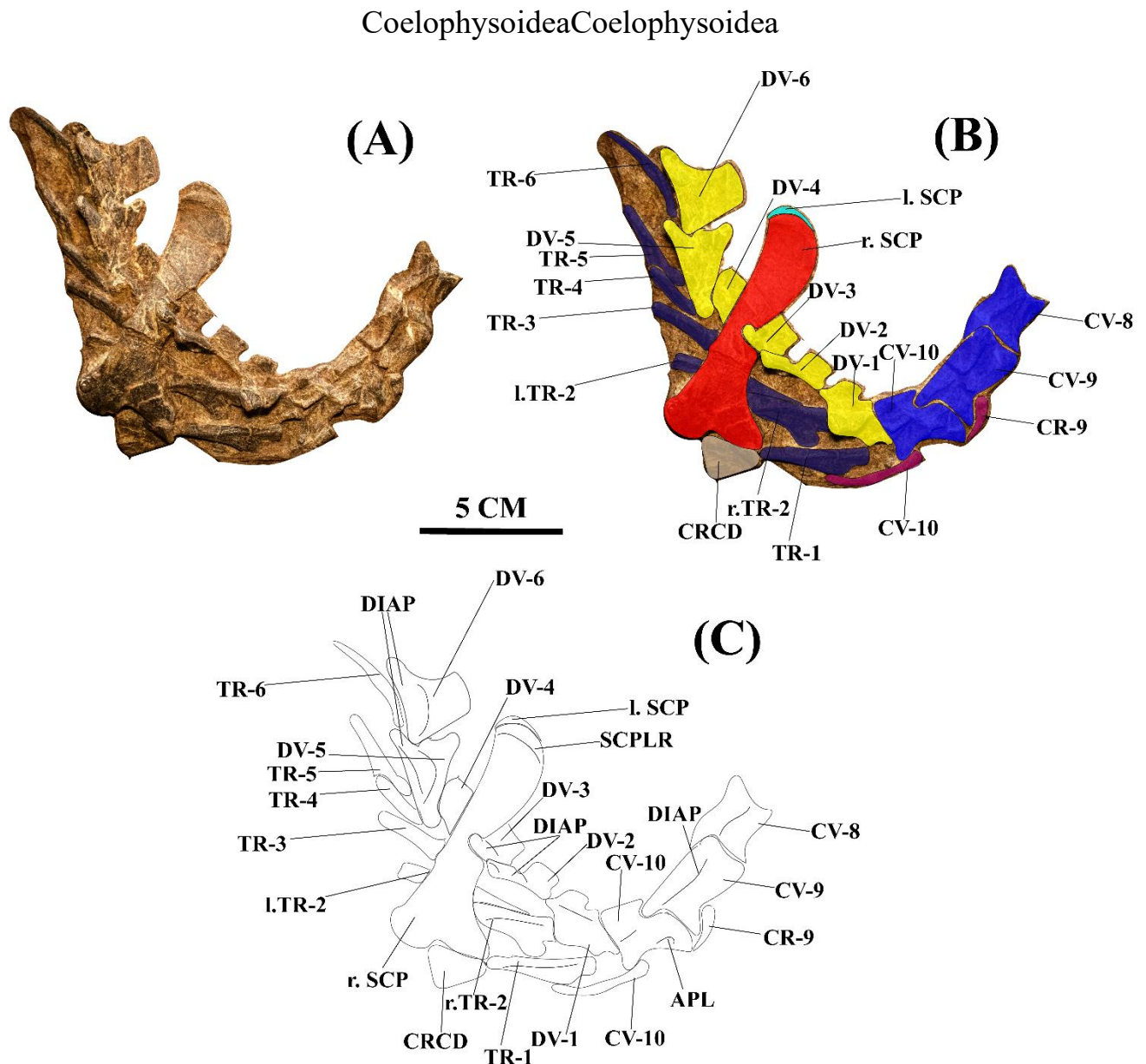


**Figure 4.5.** The vertebrae column from the posterior portion of cervical to the anterior portion of dorsal vertebrae (from CV-8 to DV-5) and shoulder girdle in lateral view, including the actual photo (A), the colored outline (B) and the sketch (C). Scale = 5

cm. Abbreviations: APL, anterior pleurocoel; CR, cervical rib; CRCD, coracoid bone. CV, cervical vertebrate; DV; dorsal vertebrate; DIAP, diapophyses; l. SCP, left scapula; l.TR, left trunk rib; r. SCP, right scapula; r. TR, right trunk rib; SCPLR, scapula lateral ridge; TR, trunk rib.

**(For editors and reviewers, due to the settings of Microsoft Word 2025, this picture is compressed to fit in the page. This picture is edited in Adobe Illustrator and I do provide larger version. If you have reading problems, please find the attachment file for access of larger pictures.)**

#### 4.2.2 Cervical Ribs

The preservation of cervical ribs is poor, while the lab repairing made details hard to observe. Among all preserved elements, the cervical ribs III, IV and VI are most distinct. Three cervical ribs are closely articulated with corresponding cervical vertebrate, and their length basically matches as well. Cervical rib VI only preserved the proximal and distal end.

Taking the right cervical rib III and VI as examples. In cervical rib VI, part of the bone is lost during preparation as the mold of bone is still visible, but the tuberculum and the articular process are in great condition. In comparison with the cervical rib preserved in *C. bauri* (Colbert 1989), the tuberculum of cervical rib located more anteriorly, constructing a steep angle with the rib articular process. The height of two joints in cervical rib IV is slightly larger than the height of anterior surface of centrum in cervical vertebrate IV. In lateral view, the anterior angle region is concave. The lateral surface of the shaft of cervical ribs are convex and smooth, and the distal end narrowed towards the midline.

One putatively unique character that could be autapomorphic to *P. lufengensis* is the length of the cervical ribs subequal to or slightly longer than the anteroposterior length of the centrum of matching cervical vertebrae. In other Coelophysoidea species, the cervical ribs are significantly elongated (Raath, 1977; Colbert, 1989) and most of the later *Averostra*-line (e.g. *D. wetherilli*, Marsh and Rowe, 2020) and even *Averostra* such as *A. fragilis* (Madsen, 1976). This character could be considered as autapomorphic to *P. lufengensis*.

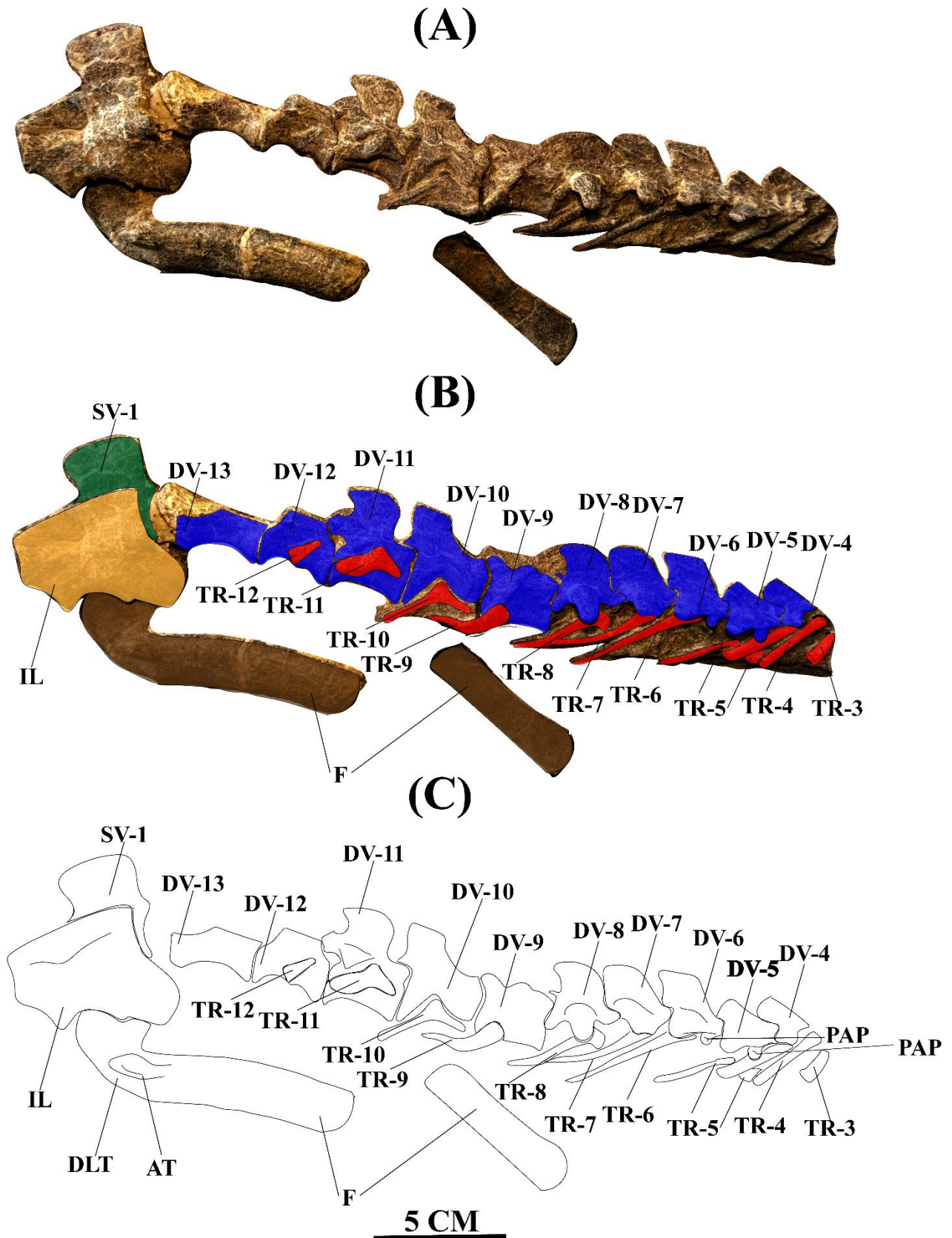


**Figure 4.6.** The picture of dorsal vertebrae column posterior to scapula and pelvic girdle in lateral view, including the actual photo (A), the colored outline (B) and the sketch (C). Scale = 5cm. Abbreviations: AT, anterior trochanter; DLT, dorsolateral

trochanter; DV, dorsal vertebrate; F, femur; IL, ilium; PAP, parapophysis; TR, trunk  
rib; SV, sacral vertebrate.

**(For editors and reviewers, due to the settings of Microsoft Word 2025, this picture is compressed to fit in the page. This picture is edited in Adobe Illustrator and I do provide larger version. If you have reading problems, please find the attachment file for access of larger pictures.)**

#### 4.2.3 Dorsal vertebrae

The dorsal portion of the vertebral column includes 13 vertebrae, exposed from right lateral view and partially dorsal view. The vertebrae column is continuously preserved, but most of the anterior dorsal vertebrae are at least partially covered by the right scapula, and the middle portion is not preserved well, which means that the dorsal vertebrae that could be measured for their length are dorsal vertebrae VIII to XIII. The length of their centrum is nearly constant throughout the series, with the variation within 2 mm, which represents the low compress rate in the posterior portion of the dorsal vertebrae. In average, the ratio between the anteroposterior length and the depth of anterior surface of centrum is 2.6, which is similar to or slightly smaller than *E. lunensis* (Serenio et al. 1993; Sereno et al. 2013), *M. rhodesiensis* (Raath 1977), *P. milnerae* (Spiekman et al. 2021), and *C. bauri* (Colbert 1989; Reinhart et al. 2009), but significantly larger than *Liliensternus liliensterni* (Ezcurra and Cuny 2007), *L. bonoi* (Martinez and Apaldetti 2017), and *D. wetherilli* (Marsh and Rowe 2020).

From lateral view, the lateral surface over centrum of vertebrae in the middle to posterior portion of the dorsal region is longitudinally depressed, and the ventral keel is absent. Although not fully exposed, the lateral margin of centrum articular rim on

the anterior and posterior side appears to be straight. The parapophyseal centroprezygapophyseal fossa is visible and well-developed over the lateral surface of the neural arch in dorsal vertebrae, which forms a deep depression ventral to diapophysis of neural spine. This is common in other early neotheropods, including *L. liliensterni* (Ezcurra and Cuny 2007), *Coelophysoidea C. bauri* (Colbert 1989), *P. triassicus* (Serenio and Wild 1992; Knoll 2008), *M. rhodesiensis* (Raath 1977), *S. kayentakatae* (Rowe 1989; Tykoski 2005), *L. bonoi* (Martinez and Apaldetti 2017), *P. milnerae* (Spiekman et al. 2021), and *Sarcosaurus woodi* (Ezcurra et al., 2020).. No distinct fossa located over the dorsal region of the diapophysis and parapophysis.

Most of the diapophysis are preserved, while the parapophysis are missing in most vertebrae. The suture between the neural arch and the centrum is closed in all vertebrae. In dorsal view, the diapophysis is complete in dorsal vertebrate from I to VIII, and their lateromedial length increases by sequence order. Starting at the dorsal vertebrate VI, the posterior border of diapophysis slightly concave. The diapophysis elongated laterally. The base and the lateral tip of diapophysis are convex, and its cross-section elliptical. At the base of the anterior border of diapophysis, the border slightly curves anteriorly towards parapophysis, showing a thin paradiapophyseal lamina, like what is observed in *M. rhodesiensis* (Raath 1977), *Lophostropheus airelensis* (Ezcurra and Cuny 2007), *P. milnerae* (Spiekman et al. 2021) and *D. wetherilli* (Marsh and Rowe 2020). In general, the structure of neural arch in LFGT-0103 shares common characters with Coelophysidae species such as *C. bauri* (Colbert 1989; Reinhart et al. 2009) and *M. rhodesiensis* (Raath 1977), but slightly different from *P. milnerae* (Spiekman et al. 2021).

The neural arches are poorly preserved and prepared in the anterior column. From dorsal view, the dorsal margin of neural spine is nearly flat, with straight anterior and posterior border that slightly tilt posteriorly. The anteroposterior length of neural spines increased dramatically starting dorsal vertebrate I and stay relatively the same from dorsal vertebrate IV. Based on dorsal vertebrae VI to XIII, the ratio between the length of neural spine versus the length of centrum is close to *C. bauri* (Colbert 1989; Reinhart et al. 2009), and *P. milnerae* (Spiekman et al. 2021), but slightly larger than Coelophysoidea *S. kayentakatae* (Rowe 1989; Tykoski 2005) and *M. rhodesiensis* (Raath 1977).

#### 4.2.4 Trunk Ribs

The trunk ribs are not preserved, and eight dorsal ribs are preserved. Most of the ribs preserved lost their distal end, and their proximal end are compressed by other bone elements. In LFGT-0103, the rib V, VI and X are demonstrated in better condition for study. In lateral view, the tuberculum of rib VI is elongated, with a relatively weakly developed centrum joint that forms a straight border between two elements. Compared to this, the tubercle joint in rib X is distinctively smaller. In rib V and X, the angle formed by anterior tubercle joint and posterior centrum joint forms a distinct deep groove along the lateral surface of rib. The shafts of the ribs are sub-elliptic in cross-section, which is different from Averostr-line neotheropods such as *S. woodi* (Ezcurra et al. 2020) and *S. sinensis* (Hu 1993). From the observation of remaining elements, the rib in LFGT-0103 matches the general paradigm of other neotheropods.

#### 4.2.5 Sacral vertebrae

The first sacral vertebrae is not obscured by the ilium laterally. Based on other Coelophysoids such as *C. bauri* (Colbert 1989), *M. rhodesiensis* (Rowe 1989) and *P. milnerae* (Spiekman et al 2021), there shall be four sacral vertebrae in *P. lufengensis*.

### 4.3 Shoulder and Forelimbs

Only the right scapula is fully preserved and exposed. The right forelimb is mostly preserved.

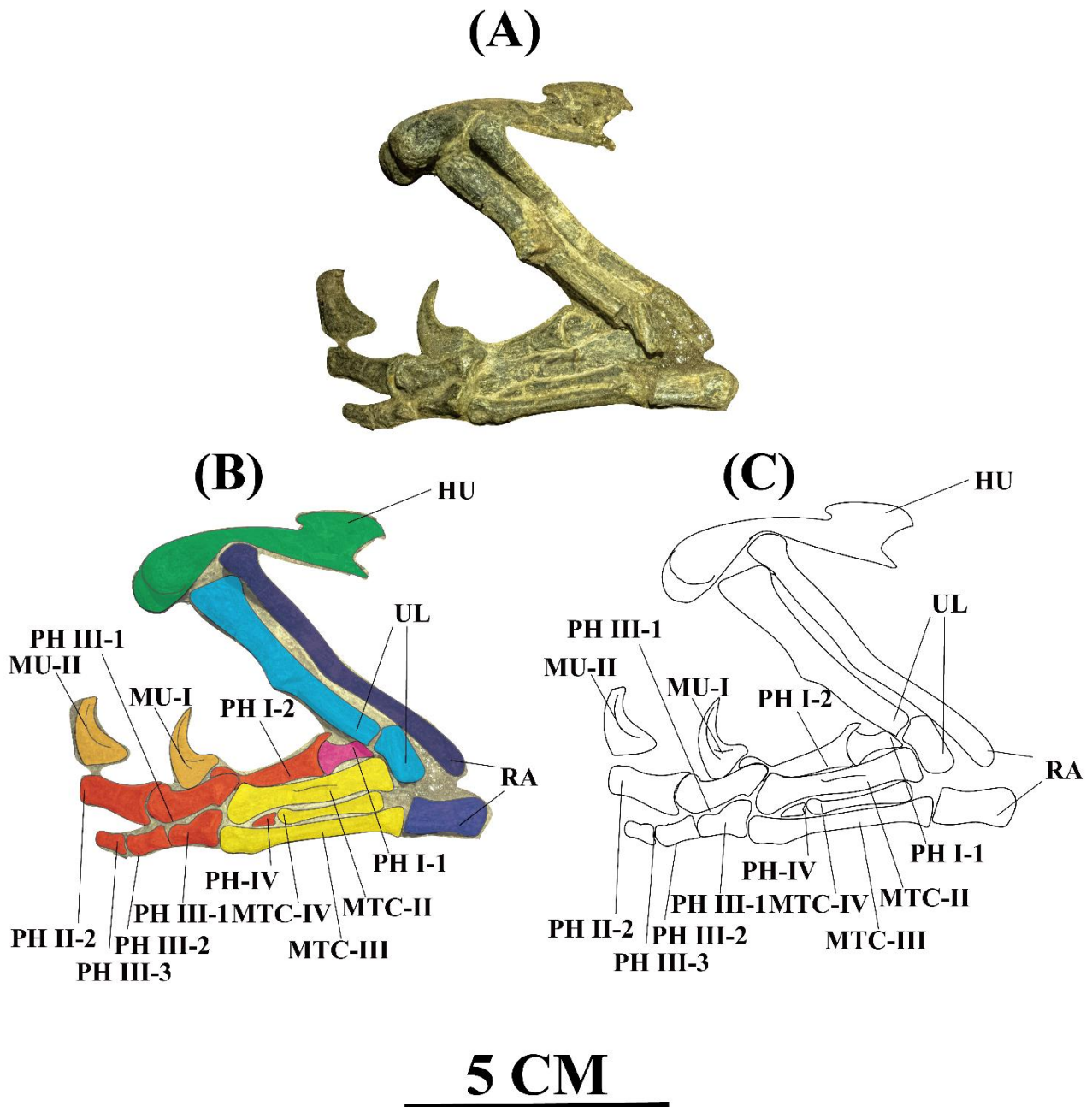


**Figure 4.7.** The forelimb of *Panguraptor lufengensis* in lateral view, including the actual picture (A), the colored outline (B) and the sketch (C) . The scale = 5 cm.

Abbreviations: HU, humerus; MTC, metacarpal; MU, manus ungual; PH, phalanges (the Roman numeral represents the manual digit, and the Arabic numeral represents the phalange); RA, radius.

**(For editors and reviewers, due to the settings of Microsoft Word 2025, this picture is compressed to fit in the page. This picture is edited in Adobe Illustrator and I do provide larger version. If you have reading problems, please find the attachment file for access of larger pictures.)**

#### 4.3.1 Pectoral Gridle

The right scapula is fully exposed in right lateral view, however, the posterior margin of the bone is not fully preserved. The total anteroposterior width of the scapula would be around 40 mm, and the dorsoventral height (measuring from the dorsal border to the lowest border of ventral processes) would be around 90 mm, making the ratio between the height to the length around 2.25. This ratio is larger than adult *C. bauri* (Colbert 1989; Reinhart et al. 2009), but much smaller than *E. murphi* (Martinez et al. 2011) and more derived *D. wetherilli* (Marsh and Rowe 2020). The narrowest point of scapula (= “scapula neck” in some research) located at the point a quarter from the ventralmost tip. In other Coelophysoidea species, the anatomy of scapula possesses a more robust scapula neck that is about a half to the widest part of scapula. In this case, LFGT-0103 shares similar pattern with Averostra-line *D. wetherilli* (Marsh and Rowe 2020) and *S. sinensis* (Hu 1993). Dorsal to the narrowest point of scapula, the scapula expands anteroposteriorly starting the dorsal margin and

reaches the widest point at about one third of the total length, then narrows down towards the narrowest point.

A distinct rounded ridge is developed over the lateral surface of the dorsal margin of scapula. In lateral view, the ridge narrows and rises from its anterior tip to its posterior end. The lateral ridge over this region of scapula in neotheropod species is the first-time record, and this character is yet to be found in other dinosaur and dinosauromorph species. In this research, this character is labeled as the autapomorphic character of *P. lufengensis*. The lateral surface of scapula ventral to the ridge is smooth and concave towards the posteroventral edge of scapula, forming a rounded anterodorsal margin in scapula. The axillary margin of scapula (=scapula blade in some research, e. g. Marsh and Rowe 2020) is straight, which is different from *C. bauri* (Colbert 1989) which possess a convex margin of scapula, but similar to Averostr-line neotheropods, including *D. wetherilli* (Marsh and Rowe, 2020).

Over the lateral surface of scapula below the fossa subscapularis, from lateral view, the glenoid fossa is well-developed, with a distinct acromion and a strong attachment for the *triceps brachii* muscle. In comparison, most neotheropods does not possess such a strong attachment for the muscle, as observed in Coelophysoidea (Raath, 1977; Colbert, 1989; Rowe, 1989), *D. wetherilli* (Marsh and Rowe, 2020), and even in Averostr such as *A. fragilis* (Madsen, 1976).

On the ventral side of the scapula, part of the coracoid bone is visible. The coracoid bone is not fused with the scapula. The glenoid fossa is not visible.

#### **4.3.2 The Forelimbs**

The right forelimb is preserved and mainly exposed from lateral view. Preserved

elements in this specimen including right humerus, ulna, radius, metacarpals and manus phalanges I – IV.

The right humerus is incomplete. The lateromedial width of the shaft narrows from proximal to distal end. The anteroposterior width of humerus is the shortest at the greater tubercle, where the cross-section of shaft becomes sub-circular instead of flat elliptical. The anterolateral tubercle is not identical in observation. At the distal end, the medial and lateral condyle is exposed mainly from distal view. Both condyles are semi-spherical in shape, with similar size, which is similar to *C. bauri* (Colbert 1989), “*C*” *rhodesiensis* (Raath 1977), and FNMH CUP-2089 (Irmis 2004), but different from Averostracine *N. frickensis* (Zahner and Brinkman 2019) and *D. wetherilli* (Marsh and Rowe 2020).

The ulna and radius are mainly exposed from lateral view, with the right radius severely broken. As observed in other neotheropods, the length of radius is gently shorter than ulna. From lateral view, the widths of the ulnar and radial shafts are similar and constant. This is different from some subadult *C. bauri* (Reinhart et al. 2009), but same with the *M. rhodesiensis* (Raath 1977). From proximal view, the olecranon of ulna is sub-triangular in shape, which matches the description of FNMH CUP-2089 by Irmis (2004). The ulnocarpal joint is preserved in LFGT-0103, however, no significant characters can be observed.

Based on the interpretation of metacarpals, the manus possesses four digits, including digits I, II, III and IV. All digits can be observed from the ventral (= palmar view in some research, e.g. Barta et al., 2017) and the lateral view. In ventral view, the width of metacarpal II is one time larger than the width of metacarpal III and IV. The

proximodistal length of metacarpal IV is smaller than a half of metacarpal II and III. Over the medial surface of metacarpal III is the slim metacarpal IV, which is shorter than metacarpal III.

The phalanx 1 of digit I is not fully exposed, but the proximodistal length of the digit I of phalange I measured from the proximal phalange articular surface to the distal phalange condyle is close to digit II phalanx I, making both phalanges longest in the manus. The ungual of digit I shares similar length with phalange II digit II, compressed lateromedially, curved ventrally as observed in other small neotheropods, and the collateral groove is visible on the lateral side. The flexor tubercle is visible on the lateral side, bounding the collateral groove mentioned above. The ungual of digit II is not fully exposed, but from the exposed lateral surface, the size of ungual on digit II is smaller than the ungual on digit I. Three phalanges of digit III could be observed, with the manual phalanx III of digit III elongated, but the ungual is missing. Only the first phalange of digit IV is visible from lateroventral view, and in previous study by You et al. (2014) and observation of other Coelophysoidea species, the distal end of digit IV is not ungual, but instead a shorten cone-shaped phalanx bone. In conclusion, the pattern of manual phalange in *P. lufengensis* is 2-3-4-1-X, which matches the record in other Coelophysoidea (Raath 1977; Colbert 1989).

#### **4.4 Pelvic Gridle**

Part of the right ilium and both ischia are preserved.

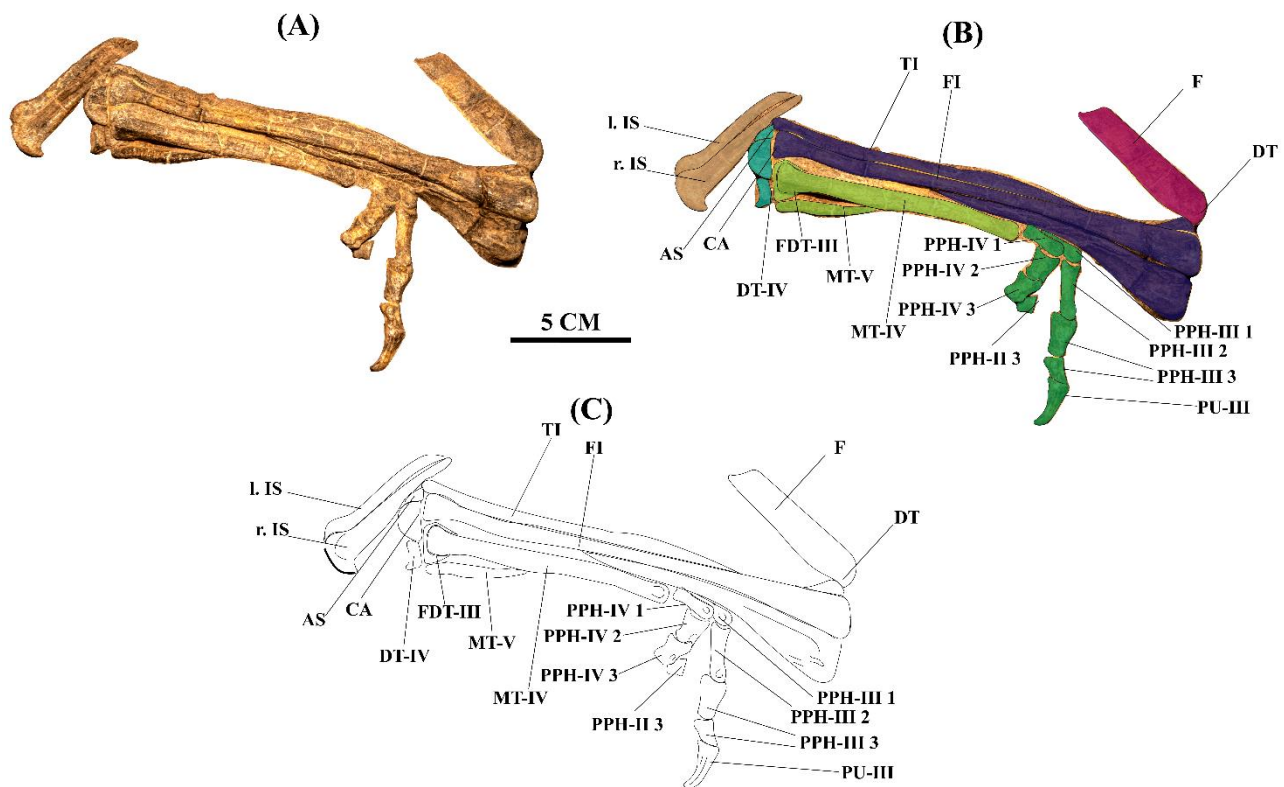


**Figure 4.8.** The picture of hindlimb of *Panguraptor lufengensis* in lateral view, with the actual picture (A), the colored outline (B) and the sketch (C). Scale = 5 cm. Abbreviations: AS, astragalus; CA, calcaneum; DT, distal tarsal; FDT, fused distal tarsal; FI, fibula; l. IS, left ischium; MT, metatarsal; PPH, phalanges of right pes (the Roman numeral represents the pedal digit, the Arabic numeral represents the phalange); TI, tibia.

**(For editors and reviewers, due to the settings of Microsoft Word 2025, this picture is compressed to fit in the page. This picture is edited in Adobe Illustrator and I do provide larger version. If you have reading problems, please find the attachment file for access of larger pictures.)**

#### 4.4.1 Ilium

The right ilium of LFGT-0103 is only exposed in the lateral view. However, based on a group of old photos acquired from Dr. Hailu You, it is demonstrated in at

least one photo that at some point before 2011 the ilium was removed from the skeleton and fixed into a complete specimen. In remaining photos, the restoration of right ilium was based on the modular paradigm of neotheropods. In this research, the description of ilium will be based on both the current situation of ilium and the photos.

Only the middle portion of ilium is preserved, which includes most of the acetabular region from preacetabular process to antitrochanter. From lateral view of LFGT-0103 and the photos, the preacetabular process in LFGT-0103 is elongated and narrowed to a point anteriorly, the dorsal rim of iliac blade is slightly convex, The lateral surface of ilium dorsal to acetabular rim is smooth and gently concave, which is observed in other neotheropods, such as the concave surface observed in Coelophysoidea species *S. kayentakatae* (Rowe, 1989), .

In lateral view, the pubic peduncle is stronger and more developed than ischiatic peduncle, which is common among Coelophysoidea (Raath 1977; Colbert 1989; Rowe 1989; Martinez and Apaldetti, 2017; Ezcurra 2017; Spiekman et al. 2021).

In recovered pictures, from medial view, the dissection shape of both the pubic peduncle is sub-triangular. The anteroposterior width of pubic peduncle remains basically the same dorsoventrally. On the contrary of this, the ischiatic peduncle is blade-shaped at the posterior end, expanding into sub-rectangular dissection in the middle with an expansion in width. In *P. lufengensis*, this blade-shape of ischiatic peduncle is unique, but could be explained by deformation during fossilization. In medial view, the angle formed between both peduncles is around 70 degrees. The ischiatic peduncle is more ventrally developed, but the broken gap indicates this is highly likely be caused by deformation. The attachment scar for sacral vertebrae and

sacral rib is not preserved from medial side.

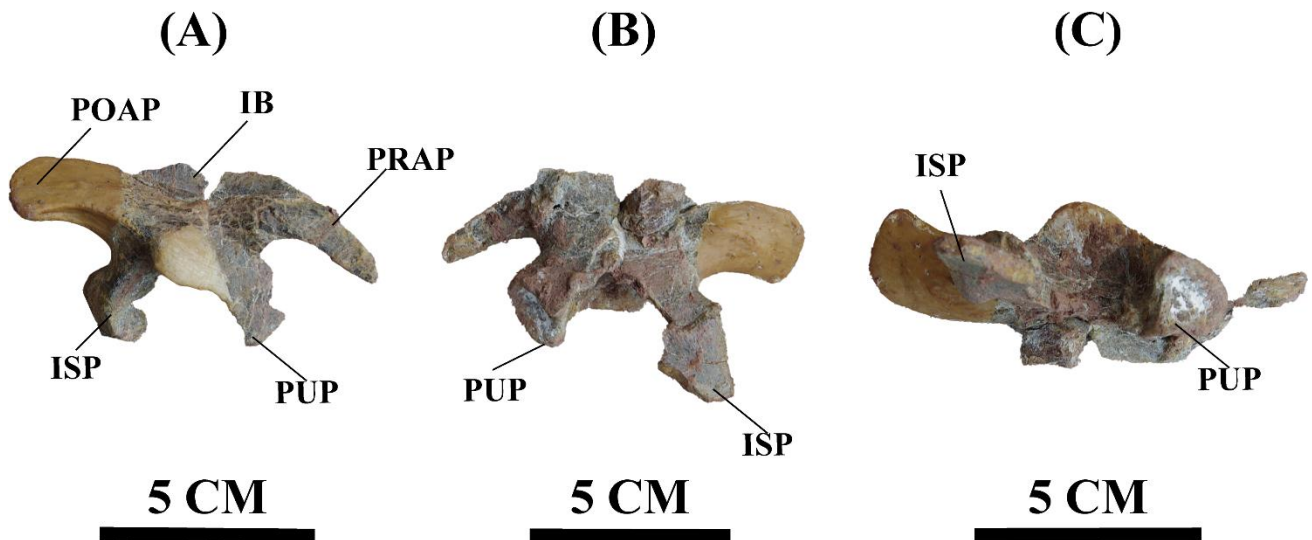


**Figure 4.9.** The picture of right ilium of *Panguraptor lufengensis* recovered from Dr. Hailu You's archive, with the lateral view (A), the medial view (B) and the ventral view (C). Scale = 5 cm. Abbreviations: IB, iliac blade; ISP, ischiatic peduncle; POAP, postacetabular process; PRAP, preacetabular process; PUP, pubic peduncle.

**(For editors and reviewers, due to the settings of Microsoft Word 2025, this picture is compressed to fit in the page. This picture is edited in Adobe Illustrator and I do provide larger version. If you have reading problems, please find the attachment file for access of larger pictures.)**

#### 4.4.2 Ischium

The shaft and distal end of paired ischium could be observed from the medial side of right femur. The shaft reaches the maximum width at the anterior most of the shaft, and then gradually narrowed down towards the distal end, leading to a teardrop-shaped cross-section. Both the lateral and the medial surface of ischium shaft is gently concave. The distal end of ischium only contacts each other at their medial surface. The distal end of ischium forms an enlarged boot. This is different from *M.*

*rhodesiensis* (Raath, 1977), which the distal head of ischium does not form an enlarged head at its posterior end, but similar to the distal “boot” of ischia in *D. wetherilli* (Marsh and Rowe, 2020) and *Sinosaurus spp.* (Hu, 1993).

#### 4.5 Hindlimb

In LFGT-0103, most elements of the right hindlimb are preserved. Only one digit of left pedal phalange is visible from the lateral side of ischia. The right femur is completely preserved. In posterior view of the specimen, one phalanx is visible ventral to the ischia. The femoral head is still housed in the acetabular rim of ilium, and the femoral distal end still articulates with the proximal end of tibia and fibula. The tibia and fibula are exposed mostly in lateral view and both their proximal and distal ends, with more exposure of fibula. The distal end of tibia and fibula still articulates with the proximal end of astragalus, calcaneum, fused distal tarsal III and distal tarsal IV and V. The right pes preserves the pedal digits III, IV and V.

The right femur is broken and missing a small portion at the middle part of shaft. The length of proximal part and distal part is 95.9 mm and 69.5 mm. Measuring in lateral view, the width of femoral distal condyles is 16.4 mm, the width of distal broken edge in proximal portion is 13.1 mm, while for the proximal broken edge of distal portion is 11.5 mm. In lateral view, the femoral head enlarged proximally, articulating with the pelvic girdle from the proximal, anterior, and medial side. The femoral shaft bends proximally at the level of the greater trochanter, and then bends anteriorly at the point distal to the femoral head, which is observed in other Coelophysoids (Raath 1977; Colbert 1989; Rowe 1989; Ezcurra 2017, Spiekman et al. 2021; Kirmse et al., 2023) and *D. wetherilli*, but different from *Averostra-line*

neotheropods, including *D. hanigani* (Martill et al. 2016) and *N. frickensis* (Zahner and Brinkman 2019), which the shaft is straight distally from the greater trochanter. The proximal margin of the femur is rounded. Posterior to the ligament fossa is a distinct dorsolateral trochanter. The dorsolateral trochanter is a ridge-shape structure with the direction parallel to the femoral shaft, which is similar to the femur of *M. rhodesiensis* (Raath 1977) and *P. milnerae* (Spiekman et al. 2021), but different from *C. bauri* (Colbert 1989) and *S. kayentakatae* (Rowe 1989). The ridge-shape dorsolateral trochanter in LFGT-0103 matches the flange-shape dorsolateral trochanter discussed by Griffin (2018), thus could be labeled as an intermediate level of maturity.

Over the anterolateral surface of femur, stands the anterior trochanter (=lesser trochanter, e.g. Raath 1977). In LFGT-0103, the trochanter shelf does not connect to the linea intermuscularis caudalis in lateral view, indicating it's far from reaching skeletal maturity, but the presence of the shelf itself indicates the individual is not juvenile, either. Comparing the femur in LFGT-0103 to the result concerning the ontogeny of neotheropods in Chinsamy, 1990, Reinhart et al., 2009, Griffin, 2018, Griffin, 2019, Spiekman et al. 2019 and Barta et al. 2022, it is reasonable to assume that LFGT-0103 demonstrates the characters of an intermediate level between juvenile and full maturity.

The femoral shaft is gently convex anteroposteriorly, with the width at anterior side basically equals to the width proximal to dorsolateral trochanter and gradually reduced towards the distal end, which is similar to what is observed in *C. bauri* (Colbert 1989), *M. rhodesiensis* (Raath 1977), *S. woodi* (Ezcurra et al. 2020), *L. liliensterni* (Ezcurra and Cuny 2007) and *D. wetherilli* (Marsh and Rowe 2020). In

lateral view, the distal end is round in outline, and the lateral condyle is directly connected to the shaft. In distal view, the lateral condyle is sub-triangular in shape. The medial condyle is unable to observe. In LFGT-0103, the distal end of femur shares same condylar structures as in FNMH CUP-2090 preserved in Field Museum of Chicago (Irmis 2004), but different from FNMH CUP-2090 as the size of femur in LFGT-0103 is much larger. In lateral view, the lateral condyle of femur possesses a fossa on the lateral side and shows as a circular-shaped distal margin. This is similar to other Coelophysoidea (Raath,1977; Colbert, 1989; Hunt et al., 1989; Rowe,1989; Spiekman et al., 2021).

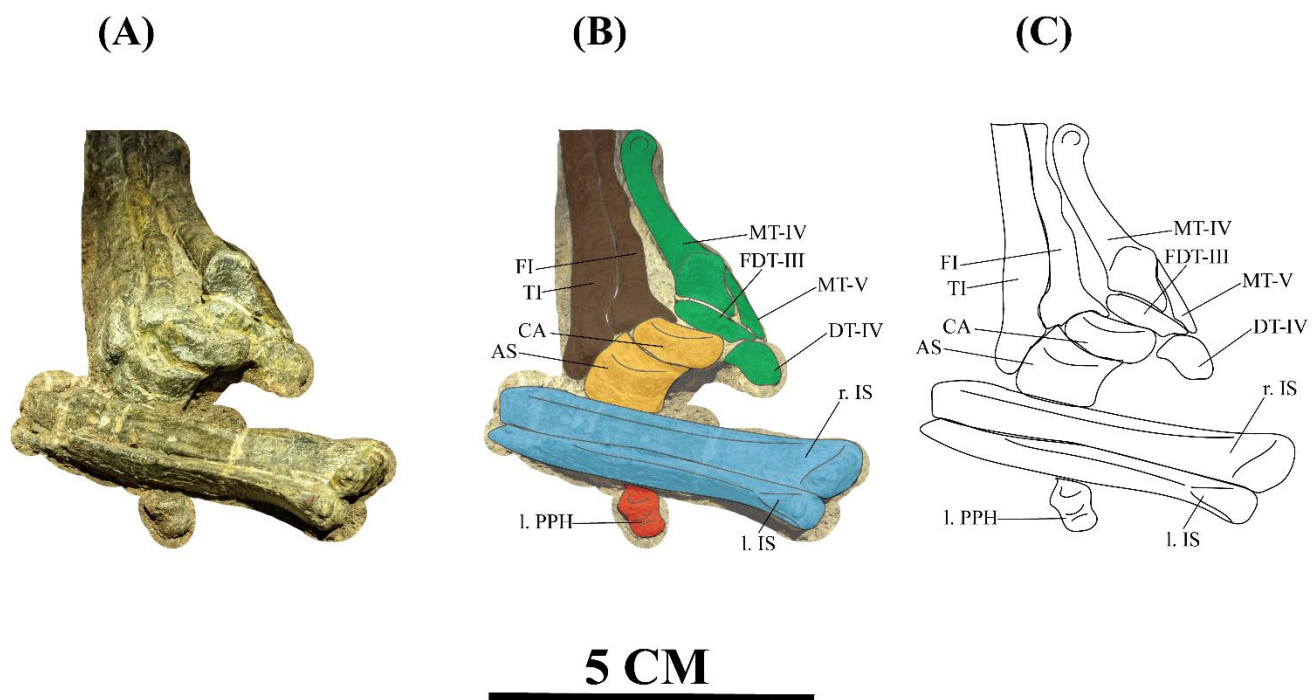


**Figure 4.10.** The hindlimb of *Panguraptor lufengensis* in posterior view, with the actual picture (A), the colored outline (B) and the sketch (C). Scale = 5 cm.

Abbreviations: lowercase l. / r., left / right; AS, astragalus; CA, calcaneum; DT, distal tarsal; FDT, fused distal tarsal; FI, fibula; IS, ischium; MT, metatarsal; PPH, pedal phalanx; TI, tibia.

**(For editors and reviewers, due to the settings of Microsoft Word 2025, this**

**picture is compressed to fit in the page. This picture is edited in Adobe Illustrator and I do provide larger version. If you have reading problems, please find the attachment file for access of larger pictures.)**

The fibula is broken into three pieces. The length of the proximal section is 19.6 mm, the shaft section is 114.9 mm, and the distal section is 34.7 mm. The estimated complete length of fibula is about 170 to 175 mm. The tibia is slightly longer than the fibula, with the length of exposed region of 179.9 mm. In proximal view, the cross-section of fibula proximal end is C-shape in projection, with an anteroposterior groove which could be possible for articulating with the distal lateral condyle of femur over the surface. The proximal end of tibia is also sub-triangular, and when both proximal ends articulate, two elements together form a sub-rectangular shape articular that articulates with the distal end of femur. The anteroposterior length of tibiofibular proximal articulate surface is 36 mm, and the lateromedial width of the surface is 33.7 mm. Measuring at the midpoint of both elements, the anteroposterior width of fibula proximal end is 24.8 mm, when it comes to the fibular shaft, the width is 6.8 mm, and the distal end is 11 mm. The distal end of fibula is much smaller than the proximal end, which is common among Coelophysoidea, as observed in specimens of mature *C.bauri* (Colbert, 1989) and *S. kayentakatae* (Rowe, 1989) . The anteroposterior width of tibia proximal end is 33.7 mm, and the distal end is 16.1 mm. The distal end of tibia is not fully exposed for measuring. The fibular crest is presented over the anteromedial side of the tibia proximal end, which possesses a groove between the crest and the proximal surface. In lateral and the proximal view, the hook-shape fibular crest is strongly developed, which is the same as what is observed in *P. podocitus* (Ezcurra

2017). The shafts of both tibia and fibula are nearly straight. The major difference between LFGT-0103 and *C. bauri* is that the fibular crest in LFGT-0103 is sharper and more developed than what is observed in *C. bauri* (Colbert 1989). The tibia and fibula in LFGT-0103 matches the character described in FNMH CUP-2090 (Irmis 2004) and also in *M. rhodesiensis* (Raath 1977), *C. arizonensis* (Ezcurra and Brusatte 2011) and *S. kayentakatae* (Rowe 1989).

Observing from the distal end of tibiofibular, the lateral surface and partial distal end of the astragalocalcaneum is observable. The exposed lateral surface is semilunate, and the anterior ligament fossa is clearly visible over the surface. The lateral end of the calcaneum is also exposed, which develops a relatively shallow groove over its surface. Beside these elements, part of the proximal end of fused distal tarsal III and distal tarsal IV are exposed, with a diagonal groove developed over the lateral surface of fused distal tarsal IV's proximal end. All the elements are not fused together, not only the astragalus and calcaneum are not fused together into astragalocalcaneum, but also the proximal and distal tarsals to metatarsals. This demonstrates a young stage of ontogeny as stated by Griffin (2018), and contradicts what is observed in the femur. In proximal view, the proximal end of distal tarsal IV possesses a sub-triangular hook structure, which is mentioned in earlier research by You et al. (2014) and listed as part of the diagnostic character. After careful research, this is autapomorphic to *P. lufengensis* in neotheropods. Similar structure is observed in *D. wetherilli* (Marsh and Rowe, 2020), but the proximal end of distal tarsal IV in *D. wetherilli* does not form a hook structure but possess a strongly pointed margin instead.

The right pes is preserved well, however, only metatarsals IV and V, a part of pedal phalange III and the complete pedal phalange IV are exposed enough for meaningful description. The complete length of metatarsal IV is 99.5 mm, for metatarsal V is 40.8 mm. The ratio between the length of metatarsal V and metatarsal IV is 2.46, which is close to *C. bauri* (Colbert 1989). The proximal end of metatarsal IV is sub-triangular, and the lateral surface of metatarsal IV is an elongated subtrapezoidal, which the margin narrows toward the posterior end. The development of metatarsal V in LFGT-0103 is common among small neotheropods, including *C. bauri* (Colbert 1989) and other neotheropods, but rare among middle- to large-size neotheropods such as *D. wetherilli* (Marsh and Rowe, 2020).

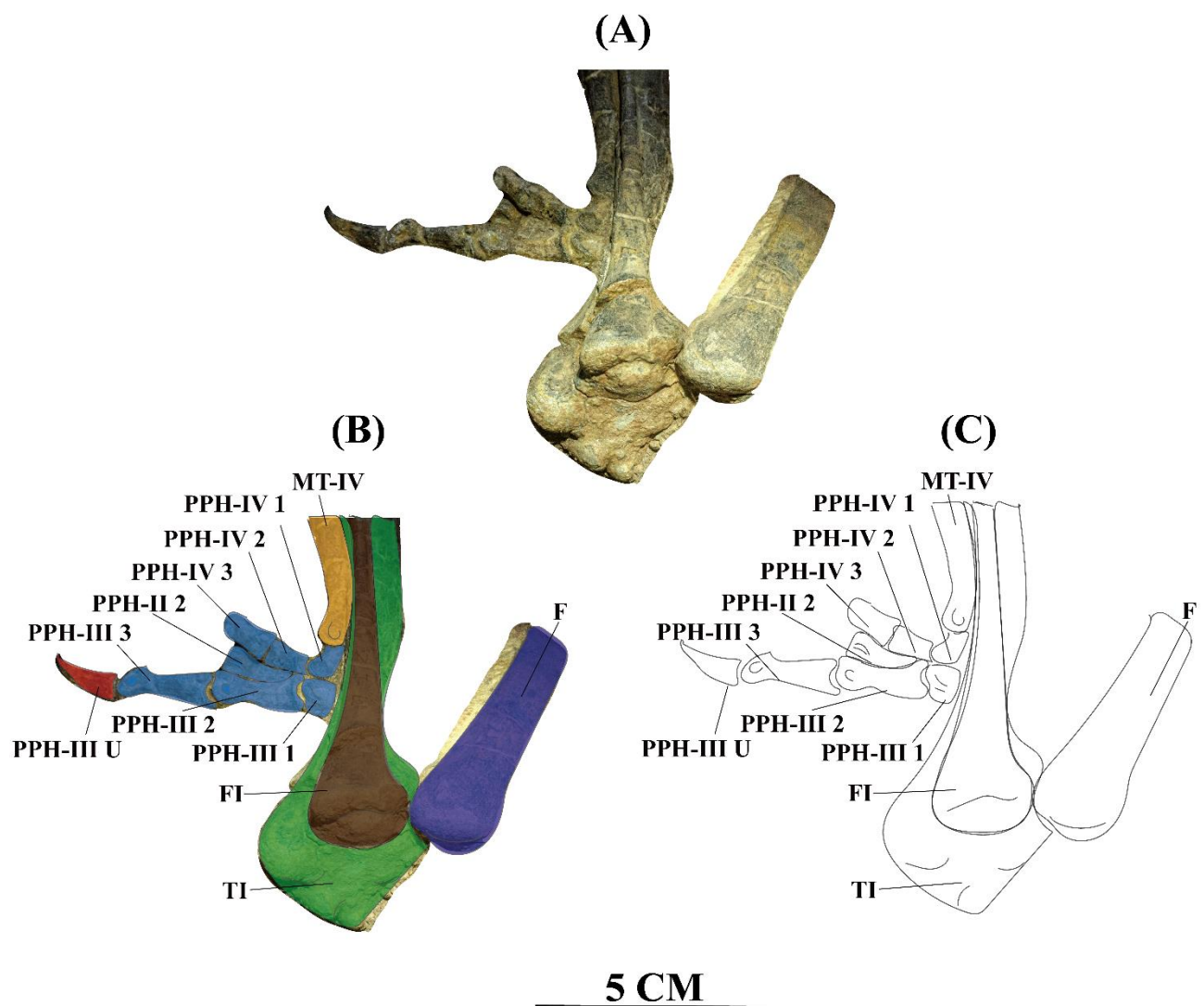


**Figure 4.11.** The picture of hindlimb of *Panguraptor lufengensis* in anterior view, with the actual picture (A), the colored outline (B) and the sketch (C). Scale= 5 cm. Abbreviations: F, femur; FI, fibula; I. MT, metatarsal; PPH, phalanges of right ped (the Roman numeral represents the pedal digit, the Arabic numeral represents the phalange); TI, tibia.

**(For editors and reviewers, due to the settings of Microsoft Word 2025, this picture is compressed to fit in the page. This picture is edited in Adobe Illustrator and I do provide larger version. If you have reading problems, please find the attachment file for access of larger pictures.)**

Both the pedal digits III and IV preserved four phalanges, including the ungual in digit III but not digit IV. Medial to the phalanx IV-1, the distal condyle of a phalange is visible, which could be the phalange I of pedal digit II based on its position. A deep groove carved between the distal condyles of phalange I of pedal digit II, with deep ligament fossa on the lateral side. The length of the three phalanges preserved in pedal digit III besides the ungual is 19.9 mm, 13.4 mm and 13.4 mm, while the length of the three phalanges in pedal digit IV is 27.1 mm, 24 mm and 21.6 mm. The ratio between the total length of three phalanges of pedal digit III versus pedal digit IV is 0.64, which is slightly smaller than *C. bauri* (Colbert 1989) and *M. rhodesiensis* (Raath 1977), indicating a larger difference in length between two pedal digits. The length of ungual of pedal digit III is 16.7 mm. Phalanges 2 and 3 of pedal digit III are partially exposed laterally, showing that the ventral width of distal condyles is larger than dorsal width and the phalanx had a sub-circular shaft. There is only one groove visible

over the lateral surface of the ungual of pedal digit III. In all the phalanges of pedal digit IV, the width of proximal articular surface is only slightly larger than that of the distal condyles, and the shaft narrowed proximally to the condyles, with a width only slightly smaller than the distal end. What is observed in LFGT-0103 is similar to what is observed in *C. bauri* (Colbert 1989) and *M. rhodesiensis* (Raath 1977), as in both species, the pedal phalanges demonstrate similar patterns in development.

## 5. Phylogenetic Analysis

The phylogenetic analysis found twelve MPTs of 1483 steps with a CI of 0.319 and a RI of 0.665. Based on the conclusion from earlier research (Goloboff et al., 2003; Ezcurra, 2024), this matrix is better optimized when an implied weight concavity K=12 is applied. Within the strict consensus tree (SCT) generated from the MPTs, the position of *P. lufengensis* locates as the earliest derived member within Coelophysoidea, while a polytomy is formed between *Powellvenator podocitus*, *Lucianovenator bonoi*, *Pendraig milnerae*, and *Syntarsus kayentakatae* within Coelophysoidea. The trees were subjected to Bremer resampling, symmetric resampling, and GC bootstrap resampling. In all three resampling results, the clade Coelophysoidea is stable as a single clade, but the relationship between species varies. All differences are between *P. podocitus*, *L. bonoi*, *P. milnerae*, and *S. kayentakatae*. The structure of polytomy formed by these groups varied as the position of *S. kayentakatae* varied. This instability does not affect the position of *P. lufengensis*, which the result matches Kirmse et al. (2023) and Ezcurra et al. (2023), but does not agree with You et al. (2014) and Griffin (2019). Besides the fact that the incomplete specimen of *P. podocitus*, *L. bonoi* and *P. milnerae* provides low level of data, there is

a good potential that at least one ghost lineage within Coelophysidae is yet to find to give a root for the polytomy.

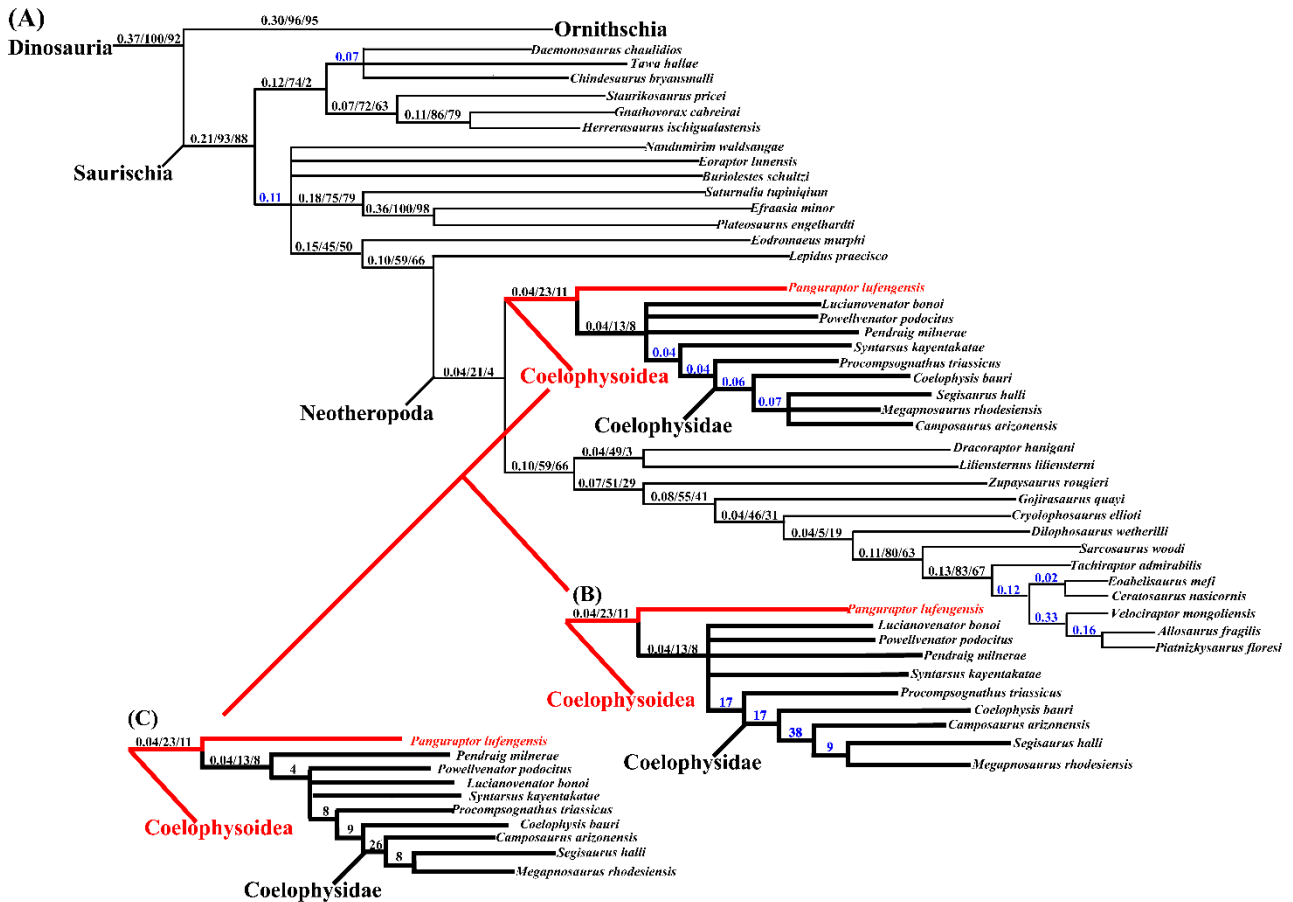


**Figure 5.1.** The SCT recovered from reconstructed when implied K=12. (A)

demonstrates the result resampled by Bremer method, (B) demonstrates the result of clade Coelophysoidea resampled by symmetrical method, (C) demonstrates the same clade resampled by GC bootstrap. In all three photographs, the single number labeled on each clade represents the support value under each resampling method. For clades

labeled with multiple numbers, the order goes by Bremer, symmetric and GC Bootstrap.

**(For editors and reviewers, due to the settings of Microsoft Word 2025, this picture is compressed to fit in the page. This picture is edited in Adobe Illustrator and I do provide larger version. If you have reading problems, please find the**

**attachment file for access of larger pictures.)**

According to the strict consensus, the following synapomorphies support *P. lufengensis* as a part of Coelophysoidea: the pneumatic features of cervical vertebrae (= pleurocoels) in the posterior portion of the centrum is present as a blind rimmed depression (129: 1); the dorsal margin dorsal to the supraacetabular rim of ilium is flat (200: 1); dorsolateral margin of the proximal portion of femur is a rounded ridge (=dorsolateral trochanter of some) (2) (230: 2); Angle between the ascending and horizontal processes of the maxilla is less than 35°(316: 1) and the length of anterior and mid-dorsal vertebral centrum is more than two times centrum height (328: 1).

According to the SCT, following synapomorphies are presented in other *P. lufengensis* but not demonstrated in Coelophysoidea are: the amount of maxillary tooth in *P. lufengensis* is less than 12, while other Coelophysoidea species possess more than 12 teeth (17: 2→0); the posterior extent of the maxillary tooth row in *P. lufengensis* is completely antorbital, while others extends to approximately half of the antero-posterior length of the orbit (18: 0→1); the attachment of the m caudifemoralis in ilium is absent in *P. lufengensis*, while in other Coelophysoidea species the attachment is distinctly presented as a deep fossa on the ventral surface of postacetabular part of the ilium (196: 2→0); the posterolateral process (= lateral malleolus) of the distal portion in tibia in *P. lufengensis* present and extends distinctly beyond the level of the lateral margin of the facet for the reception of the ascending process of astragalus, as in other Coelophysoidea species, this portion of tibia is present and extends distinctly beyond the level of the lateral margin of the facet for the reception of the ascending process of astragalus (254: 2→1); in *P. lufengensis*, the

anteroposterior depth of the distal end compared with that of the proximal end is considerably lower, with a distal depth lower than 50% that of the proximal end, whereas in other Coelophysoidea species, the depth is lightly lower . (354: 1→2); and the iliac pubic peduncle ventral extension is more distinctly more ventrally extended than the ischiadic peduncle, whereas in Coelophysoidea species it is either similar to ischiadic peduncle or more ventrally extended (388: 0/1→1).

The synapomorphy support the clade that consists of all other Coelophysoids excluding *Panguraptor* are: the lateral surface of the iliac postacetabular process has distinct posterior rim for the origin of the M. iliofibularis (341: 1); the posterolateral process (= lateral malloelus) of tibia in anterior or posterior view is either lobular or tabular (342: 0/1); and, in proximal view, the posterior margin of the metatarsal IV possesses a short, posteromedial apex (364: 1).

In all the reconstructions, no matter which resampling method is used, the relationship between members in clade (family Coleophysidae) is stable, composed of clade *Coelophys bauri*, *Camposaurus arizonensis*, *Segisaurus halli* and *Megapnosaurus rhodesiensis*. The synapomorphic character shared by family Coleophysidae is the anteromedial corner of the femoral distal end is either squared off near 90 degree or acute (= larger than 90 degree) (247: 1).

## 6. Conclusion

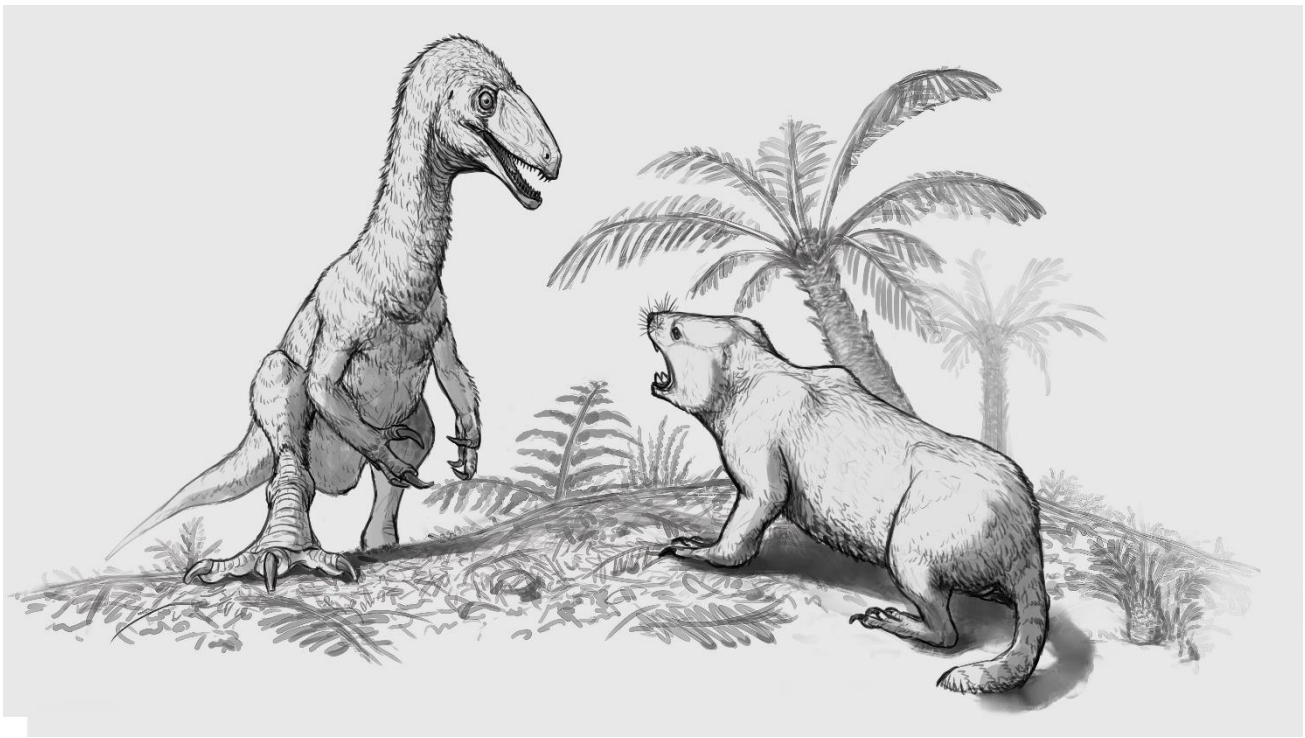


**Figure 6.1.** Life reconstruction of *P. lufengensis* confronting an individual of synapsid *Bienotherium*. Artwork By Jianping Jin from Greenhouse Revolution Studio.

Based on this research, after carefully examining the holotype of *Panguraptor lufengensis* and its new description, the autapomorphies of *P. lufengensis* were re-examined, expanding to a combination of six characters for its diagnostic characters.

The new phylogenetic analysis including the new information on *Panguraptor* recovers the position of *P. lufengensis* within superfamily Coelophysoidea as the earliest-diverging clade. This result matches the previous analysis in Kirmse et al., 2023 and Ezcurra et al., 2023.

In conclusion, *P. lufengensis* demonstrates a share set of common patterns of Coelophysoidea members in postcranial skeleton. The alternative resolution of the tree generated during the different method of resampling could be interpreted as a fact that *P. lufengensis* resembles a ghost lineage that derived from other Coelophysoidea at

very early stage and evolved separately in nowadays East Asia region. Along with the biogeographic contribution of Coelophysoidea and the geological background of the breakdown of supercontinent Pangea, it is highly possible that the diversification among major groups within Coelophysoidea occurs much earlier than fossil record.

Need to mention by the end, in last five years, field research discovered a new dinosaurian fauna in Yunnan and Sichuan Province, including several unnamed Coelophysoidea specimens and complete skeletons from different sediments. Taking this into consideration, it is highly likely that the evolution of Coelophysoidea had taken an independent routine in East Asia.

## **7. Acknowledgements**

We particularly thank our international colleagues, Krishna Hu from Institute of Paleontology and Paleoanthropology of Chinese Academy of Science (IVPP) and João Pedro Silva Kirmse from Ludwig-Maximilians-Universität in Munich, for their offering of information on materials in North America and Europe has aided the comparison between different Coelophysoidea species. We thank Dr. William Simpson from Field Museum of Chicago and Dr. Maureen Walsh from Natural History Museum of Los Angeles for their kindly giving us access to their specimen collections. We thank Dr. Xinxin Ren from Institute of Geology of Chinese Academy of Geological Sciences and Dr. Qiannan Zhang and Dr. Paul Rummy from IVPP for their suggestions on the fine tuning of this research. We thank World Dinosaur Valley and Dinosaur Fossil Research and Protection Center of Lufeng City, Chuxiong Yi Autonomous Prefecture, Yunnan Province for their grant of access of their specimens and their resources, and with special thanks to Yongbin Liang, Jiayou Luo, Shubiao

Yue, Yong Wang from World Dinosaur Vally and Shuyong Yue, Shukai Yue, Shuchun Yue, and Zhu from Dinosaur Fossil Research and Protection Center whom offered tremendous help during the research. We thank Jianping Jin and Xin Yu from Greenhouse Revolution Studio of Beijing Hanpinhui Technology Co., Ltd. for their dedication in the artwork of life reconstruction. This work was supported by the National Natural Science Foundation of China (42288201 and 42372030).

### **Funding Information**

This work was supported by the National Natural Science Foundation of China (42288201 and 42372030).

### **Declarations**

**Ethics approval and consent to participate:** Not applicable.

**Consent for publication:** Not applicable.

**Competing interests:** The authors declare no competing interests

**Zechuan Zhang is the corresponding author of this research. E-mail address:** [zhangzechuan@ivpp.ac.cn](mailto:zhangzechuan@ivpp.ac.cn)

### **Reference**

Alcober, O., & Martinez, R. (2010). A new herrerasaurid (Dinosauria, Saurischia) from the Upper Triassic Ischigualasto Formation of northwestern Argentina.

ZooKeys. 63: 55-81. DOI:10.3897/zookeys.63.550.

Averianov, A., and Lopatin, A. (2014). On the phylogenetic position of Monotremes (Mammalia: Monotremata). Paleontology Journal. 48: 426 – 446. [Original text in Russian text published in Paleontologicheskii Zhurnal 4: 83 – 104]

Bakker, R. (1986). The Dinosaur Heresies. New York: William Morrow. 481.

- Baron, M., Norman, D., Barrett, P. (2017). A new hypothesis of dinosaur relationships and early dinosaur evolution. *Nature*. 543. 501-506. doi: 10.1038/nature21700.
- Barta, D., Nesbitt, S., and Norell, M. (2017). The evolution of the manus of early theropod dinosaurs is characterized by high inter- and intraspecific variation. *Journal of Anatomy*. 232. doi: 10.1111/joa.12719.
- Barta, D., Griffin, C., & Norell, M. (2022). Osteohistology of a Triassic dinosaur population reveals highly variable growth trajectories typified early dinosaur ontogeny. *Science Report*. 12: 17321. DOI: 10.1038/s41598-022-22216-x.
- Bi, S., Wang, Y., Guan, J., Sheng, X., and Meng, J. (2014). Three new Jurassic euharamiyidan species reinforce early divergence of mammals. *Nature*. 514 (7524): 578 – 584.
- Bremer, K. (1994). Branch support and tree stability. *Cladistics*. Volume 10: 295-304.
- Buckley, L., and Currie, P. (2014). Analysis of intraspecific and ontogenetic variation in the dentition of *Coelophysis bauri* (Late Triassic), and implications for the systematics of isolated theropod teeth. *Bulletin of the New Mexico Museum of Natural History and Science*. 63: 1-73.
- Bugos, J., & McDavid, S. (2024). Immature skulls of the theropod dinosaur *Coelophysis bauri* from Ghost Ranch, New Mexico. *Acta Palaeontologica Polonica*. 69: 549-563. DOI: 10.4202/app.01085.2023.
- Camp, C. (1936). A new type of small bipedal dinosaur from the Navajo sandstone of Arizona. University of California Publishing, *Bulletin of Department of Geological Science*. 24: 39-56.
- Carrano, M., & Sampson, S. 2004. A review of coelophysoids (Dinosauria:

Theropoda) from the Early Jurassic of Europe, with comments on the late history of the Coelophysoidea. *Neues Jahrbuch für Geologie und Paläontologie - Monatshefte*. 2004 (9): 537 – 558. DOI:10.1127/njgpm/2004/2004/537.

Carrano, M., Benson, R., & Sampson, S. (2012). The phylogeny of Tetanurae (Dinosauria: Theropoda). *Journal of Systematic Paleontology*. 10(3): 599-599. DOI: 10.1080/14772019.2012.713753.

Chen, X. Y., Wang, Y. M., Zhang, Q. N., Wang, T., & You, H. L. (2025). A new species of *Xingxiulong* (Dinosauria, Sauropodomorpha) from the lower Jurassic Lufeng formation of Yunnan Province, China. *Historical Biology*, 37(12), 2800–2809. <https://doi.org/10.1080/08912963.2025.2458130>

Chinsamy-Turan, A. (1990). Physiological implications of the bone histology of *Syntarsus rhodesiensis* (Saurischia: Theropoda). *Palaeontologia Africana*. 27: 77-82.

Chow, M., and Hu, C. (1959). A new tritylodontid from Lufeng, Yunnan. *Vertebrata Palastatica* 3: 9-12. [Original text in Chinese]

Chow, M. (1962). A Tritylodont specimen from Lufeng, Yunnan. *Vertebrata Palastatica* 6: 365-367. [Original text in Chinese]

Cope, E. (1887). A Contribution to the History of the Vertebrata of the Trias of North America. *Proceedings of the American Philosophical Society*. 24 (126): 209 – 228.

Cope, E. (1889). On a new genus of Triassic Dinosauria. *The American Naturalist*. 23 (271): 626. DOI: 10.1086/274979.

Colbert, E. (1989). The Triassic Dinosaur *Coelophysus*. Museum of Northern Arizona

Bulletin. 57: 1 – 160.

Crompton, A., and Sun, A. (1985). Cranial structure and relationships of the Liassic mammal *Sinocondon*. Zoological Journal of the Linnean Society. 85: 99 – 119.

Currie, P. J., Xing, L., Wu, X., & Dong, Z. (2019). Anatomy and relationships of *Sinosaurus triassicus* (Theropoda: Coelophysoidea) from the Lufeng Formation (Lower Jurassic) of Yunnan, China. 7th Annual Meeting Canadian Society of Vertebrate Palaeontology. DOI: 10.18435/vamp29349.

Cul, G. (1976). *Yunnania*, a new tritylodontid from Lufeng, Yunnan. Vertebrata Palaeontologica 25: 1-7. [Original Text in Chinese]

Cui, G. (1981). A new genus of Tritylodontidae. Vertebrata palaeontologica. 19:5-10. [Original Text in Chinese]

Dal Sasso, C., Simone M., & Andrea C. (2018). The oldest ceratosaurian (Dinosauria: Theropoda), from the Lower Jurassic of Italy, sheds light on the evolution of the three-fingered hand of birds. PeerJ. DOI: 10.7717/peerj.5976.

Dong, Z. M. (1992). Dinosaurian Fauna of China. Beijing: China Ocean Press. 1-188.

Ezcurra, M. (2006). The cranial anatomy of the coelophysoid theropod *Zupaysaurus rougieri* from the Upper Triassic of Argentina. Historical Biology. 19:2, 185 – 202. DOI: 10.1080/08912960600861467

Ezcurra, M., & Cuny, G. (2007). The Coelophysoid *Lophostropheus airelensis*, gen. nov.: A review of the systematics of “*Liliensternus*” *airelensis* from the Triassic – Jurassic outcrops of Normandy (France). Journal of Vertebrate Paleontology. 27(1): 73-86. DOI: 10.1671/0272-4634(2007)27[73:tclagn]2.0.co;2.

- Ezcurra, M. & Brusatte, S. (2011). Taxonomic and phylogenetic reassessment of the early neotheropod dinosaur *Camposaurus arizonensis* from the Late Triassic of North America. *Palaeontology*. 54(4), 763-772.
- Ezcurra, M., Fiorelli, L., Martinelli, A., & Rocher, S. (2017). Deep faunistic turnovers preceded the rise of dinosaurs in southwestern Pangaea. *Natural Ecology and Evolution*. 1477-1484. DOI: 10.1038/s41559-017-0305-5.
- Ezcurra, M. (2017). A New Early Coelophysoid Neotheropod from the Late Triassic of Northwestern Argentina. *Ameghiniana*. Volume 54 (5): 506 – 538. doi: 10.5710/AMGH.04.08.2017.3100
- Ezcurra, M., Butler, R., Susannah M., Sansom, I., Meade, L., & Radley, J. (2020). A revision of the early neotheropod genus *Sarcosaurus* from the Early Jurassic (Hettangian – Sinemurian) of central England. *Zoological Journal of the Linnean Society*. Volume 191 (1), 113 – 149. doi: 10.1093/zoolinnean/zlaa054.
- Ezcurra, M., Marke, D., Walsh, S., & Brusatte, S. (2023). A revision of the ‘coelophysoid-grade’ theropod specimen from the Lower Jurassic of the Isle of Skye (Scotland). *Scottish Journal of Geology*. 2023. Volume 59.
- Ezcurra, M. (2024). Exploring the effects of weighting against homoplasy in genealogies of palaeontological phylogenetic matrices. *Cladistics*. 40: 242-281. DOI: 10.1111/cla.12581.
- Fraas, E. (1913). Die neuesten Dinosaurierfunde in der schwäbischen Trias. *Naturwissenschaften* 1(45): 1097-1100.
- Goloboff, P., Farris, J., Källersjö, M., Oxelman, B., Ramírez, M., & Szumik, C. (2003). Improvements to resampling measures of group support. *Cladistics*. 19:

324-332. DOI: 10.1016/S0748-3007(03)00060-4.

Goloboff, P., & Morales, M. (2023). TNT version 1.6, with a graphical interface for MacOS and Linux, including new routines in parallel. *Cladistics*. 2023. 39 (2). 144-153. DOI: 10.1111/cla.12524.

Griffin, C. (2018). Developmental patterns and variation among early theropods. *Journal of Anatomy*. 2018. 232: 604-640. DOI: 10.1111/joa.12775.

Griffin, C. (2019). Large neotheropods from the Upper Triassic of North America and the early evolution of large theropod body sizes. *Journal of Paleontology*. 93:1010 – 1030. DOI:10.1017/jpa.2019.13.

Harris, J., Lucas, S., Estep, J., and Li, J. (2000). A new and unusual sphenosuchian (Archosauria: Crocodylomorpha) from the Lower Jurassic Lufeng Formation, People's Republic of China. *Neues Jahrbuch für Geologie und Paläontologie - Abhandlungen*. 215: 47-68. doi: 10.1127/njgpa/215/2000/47.

Hai, L., Wang, Y., Wang, H., Gao, Y., Zhu, Z., You, H., and Wang, Y. (2025). A juvenile specimen of *Sinoconodon rigneyi* with new information on pattern of tooth replacement. *Journal of Vertebrate Paleontology*. 44. doi: 10.1080/02724634.2024.2442473.

Hendrickx, C., Hartman, S., & Mateus, O. (2015). An Overview of Non-Avian Theropod Discoveries and Classification. – *PalArch's Journal of Vertebrate Palaeontology* 12, 1 (2015), 1-73. ISSN 1567-2158.

Holtz, T. R. (1994). The Phylogenetic Position of the Tyrannosauridae: Implications for Theropod Systematics. *Journal of Paleontology*, 68(5), 1100 – 1117. <http://www.jstor.org/stable/1306180>

- Hu, S. (1993). A New Theropoda (*Dilophosaurus sinensis* SP. NOV.) From Yunnan, CHINA. *Certebrata Palasiatica*. 31(1). 65-69.
- Hunt, S., Lucas, A., Heckert, R., and Lockley, M. (1989). Late Triassic dinosaurs from the western United States. *Géobios*. 31(4): 511-531.
- Hsiou, A., Franca, M., and Fergolo, J. (2015). New data on the *Clevosaurus* (Sphenodontia: Clevosauridae) from the Upper Triassic of southern Brazil. *PloS ONE*. doi: 10.1371/journal.pone.0137523.g002.
- Jones, M. (2006). “The Early Jurassic *Clevosaurus* from China (Diapsida: Lepidaosauria).” In Harris, J., Jerry, D., Lucas, S., Spielmann, J., Lockley, M., Milner, A., Kirkland, J. et al. *The Triassic-Jurassic Terrestrial Transition*. New Mexico Museum of Natural History and Science Bulletin. 37: 548 – 562.
- Kielan-Jaworoska, Z., Cifelli, R., and Luo, Z. (2004). *Mammals from the Age of the Dinosaurs: Origin, Evolution, and Structure*. New York: Columbia University Press. 1 – 630.
- Kirmse, J., Benton, M., Hildebrandt, C., Langer, M., & Marsola, J. (2023). A Coelophysoidea (Dinosauria, Theropoda) femur from the Tytherington fissures (Rhaetian, Late Triassic), Bristol, UK. *Proceedings of the Geologists Association*. DOI: 10.1016/j.pgeola.2023.07.005.
- Knoll, F. (2008). On the *Procompsognathus* postcranium (Late Triassic, Germany). *Geobios*. 41: 779-786.
- Langer, M., Novas, F., Bittencourt, J., Ezcurra, M., and Gauthier, J. (2020). Dinosauria. In *Phylonoms: a companion to the PhyloCode* (eds K de Queiroz, PD Cantino, JA Gauthier), pp. 1209–1217. Boca Raton, FL: CRC Press.48.

- Li, H., Xu, X., Jiang, J., Liu, J., Brusatte, S., and Bi, S. (2025). New material of a non-averostran neotheropod dinosaur from the Lower Jurassic Lufeng Formation of Yunnan, south-western China. *Zoological Journal of the Linnean Society*. Volume 204 (I). DOI: 10.1093/zoolinnea/zlaf034.
- Luo, Z., and Sun, L. (1993). *Oligokyphus* (Cynodontia: Tritylodontidae) from the Lower Lufeng Formation (lower Jurassic) of Yunnan, China. *Journal of Vertebrate Paleontology*. 13 (4): 477-482.
- Luo, Z. (1994). "Sister-group relationships of mammals and transformations of diagnostic mammalian characters." In Fraser et al., *In the Shadow of the Dinosaurs: Early Mesozoic Tetrapods*. Cambridge: Cambridge University Press. 98 -128.
- Luo, Z., and Wu, X. (1994). *In the Shadow of the Dinosaurs—Early Mesozoic Tetrapods* (eds Fraser, N. C. & Sues, H.-D.) 251–270 (Cambridge Univ. Press, 1994).
- Luo, Z., Lucas, S., Li, J., and Zhen, S. (1995). A new specimen of *Morganucodon oehleri* from the Lower Lufeng Formation, Yunnan, China. *Neues Jahrbuch für Geologie und Paläontologie - Abhandlungen*. 11. 671.
- Luo, Z., Crompton, A., and Sun, A. (2001). A new mammaliaform from the Early Jurassic and evolution of mammalian characteristics. *Science*. 292: 1535-150.
- Lv, J., Li, T, Zhong, S., Azuma, F., Dong, Z. M., & Ji, Q. (2007). New yunannosaurid dinosaur (Dinosauria, Prosauropoda) from the Middle Jurassic Zhanghe Formation of Yuanmou, Yunnan Province of China. *Memoir of the Fukui Prefectural Dinosaur Museum*. 6: 1 – 5.

- Mao, F., Zhang, C., Ren, J., Wang, T., Wang, G., Zhang, F., Ric,h T., Vickers-Rich, P., and Meng, J. (2024). Fossils document evolutionary changes of jaw joint to mammalian middle ear. *Nature*. Apr;628(8008):576-581. doi: 10.1038/s41586-024-07235-0.
- Marsh, A., Parker, W., Langer, M., and Nesbitt, S. (2019). Redescription of the holotype specimen of *Chindesaurus bryansmalli* Long and Murry, 1995 (Dinosauria: Theropoda) from Petrified Forest National Park, Arizona: *Journal of Vertebrate Paleontology*. 39: p. e1645682
- Marsh, A., & Rowe, T. (2020). A comprehensive anatomical and phylogenetic evaluation of *Dilophosaurus wetherilli* (Dinosauria, Theropoda) with descriptions of new specimens from the Kayenta formation of northern Arizona. *Journal of Paleontology*. 94(S78): 1-103. DOI: 10.1017/jpa.2020.14.
- Marsola, J., Bittencourt, J., Butler, R., Da Rosa, Á., Sayão, J., & Langer, M. (2019a). A new dinosaur with theropod affinities from the Late Triassic Santa Maria, South Brazil. *Journal of Vertebrate Paleontology*. 38 (5): e1531878. DOI:10.1080/02724634.2018.1531878.
- Martill, D., Vidovic, S., Howells, C., & Nudds, J. (2016). The Oldest Jurassic Dinosaur: A Basal Neotheropod from the Hettangian of Great Britain. *PLOS ONE*. 2016. 11 (1): e0145713. DOI:10.1371/journal.pone.0145713.
- Martinez, R., Alcober, O., Colombi, C., Renne, P., Montañez, I., and Currie, B. (2011). A Basal Dinosaur from the Dawn of the Dinosaur Era in Southwestern Pangaea. *Science*. 331. DOI: 206-10. 10.1126/science.1198467.
- Martinez, R., & Apaldetti, C. (2017). A Late Norian-Rhaetian Coelophysid

Neotheropod (Dinosauria, Saurischia) from the Quebrada Del Barro Formation, Northwestern Argentina. AMEGHINIANA. 2017. Volume 54 (5): 488 – 505. doi: 10.5710/AMGH.09.04.2017.3065.

Meng, J. (2014). Mesozoic mammals from China: implications for phylogeny and early evolution of mammals. National Science Review. 1: 521-542. doi: 10.1093/nsr/nwu070.

Naish, D., Cau, A., Holtz Jr., T.R., Fabbri, M., and Gauthier, J.A., 2020. Theropoda O. C. Marsh 1881 [D. Naish, A. Cau, T. R. Holtz, Jr., M. Fabbri, and J. A. Gauthier], converted clade name. In: De Queiroz, K., Cantino, P.D., Gauthier, J.A. (Eds.), Phylonyms: A Companion to the PhyloCode. CRC Press, pp. 1236–1246.

Nesbitt, S., Smith, N., Irmis, R., Turner, A., Downs, A., and Norell, M. (2009). A complete skeleton of a late Triassic saurischian and the early evolution of dinosaurs. Science. 326: 1530 – 1533.

Nopcsa, F. (1928). The genera of reptiles. Palaeobiologica. 1: 163–188. DOI: 10.1093/zoolinnean/zlaa080.

Novas, F., Agnolin, F., Ezcurra, M., Müller, R., Martinelli, A., & Langer, M. (2021). Review of the fossil record of early dinosaurs from South America, and its phylogenetic implications. Journal of South American Earth Sciences. Volume 110: 103341. DOI: 10.1016/j.jsames.2021.103341.

Patterson, B., and Olson, E. (1961). A triconodontid mammal from the Triassic of Yunnan. Pp. 129-191. in International Collection in the Evolution of Lower and Nonspecialized Mammals. Brussels: Koninklijke Vlaamse Academie voor Wetenschappen, Letteren en Schone Kunsten van België

Qvarnström, M., Wernström, J., Wawrzyniak, Z., Barbacka, M., Pacyna, G., Górecki, A., Ziaja, J., Jarzynka, A., Owocki, K., Sulej, T., Marynowski, L., Pienkowski, G., Ahlberg, P., & Niedźwiedzki, G. (2024). Digestive contents and food webs record the advent of dinosaur supremacy. *Nature*. 636. 397-403. DOI: 10.1038/s41586-024-08265-4.

Raath, M. (1977). The Anatomy of the Triassic Theropod *Syntarsus rhodesiensis* (Saurischia: Podokesauridae) and a Consideration of Its Biology. Department of Zoology and Entomology, Rhodes University, Salisbury, Rhodesia. 1 – 233.

Rauhut, O., & Hungerbühler, A. (1998). A review of European Triassic theropods. *Gaia*. 15: 75-88.

Rauhut, O., and Pol, D. (2019). Probable basal allosauroid from the early Middle Jurassic Cañadón Asfalto Formation of Argentina highlights phylogenetic uncertainty in tetanuran theropod dinosaurs. *Scientific Reports* 2019; 9:18826. doi: 10.1038/s41598-019-53672-7.

Ren, X., Su, X., Wang, G., & You, H. (2021). Sedimentological evidence suggests an Early Jurassic age for *Yunnanosaurus youngi* (dinosauria: Sauropodomorpha) in Yunnan Province of China. *Historical Biology*. 34(9), 1827-1833. doi: 10.1080/08912963.2021.1984445.

Reinhart, L. F., Lucas, S. G., Heckert, A. B., Spielmann, J. A., & Celleskey, M. D. (2009). The paleobiology of *Coelophysis bauri* (Cope) from the Upper Triassic (Apachean) Whitaker quarry, New Mexico, with detailed analysis of a single quarry block. Albuquerque, NM: New Mexico Museum of Natural History and Science.

- Rigney, H. (1963). A specimen of *Morganucodon* from Yunnan. *Nature*. 197: 1122 – 1123.
- Rowe, T. (1989). A new species of the theropod dinosaur *Syntarsus* from the Early Jurassic Kayenta Formation of Arizona. *Journal of Vertebrate Paleontology*. 9(2):125-136. doi: 10.1080/02724634.1989.10011748.
- Sekiya, T. (2010). A new prosauropod dinosaur from Lower Jurassic in Lufeng of Yunnan[J]. *World Geology*. 29(1): 6-15.
- Sereno, P., & Wild, R. (1992). *Procompsognathus*: theropod, "thecodont" or both? *Journal of Vertebrate Paleontology*. 12 (4): 435 – 458.  
DOI:10.1080/02724634.1992.10011473.
- Sereno, P., Forster, C, Rogers, R, & Moneta, A. (1993). Primitive dinosaur skeleton from Argentina and the early evolution of the Dinosauria. *Nature*. 1993. 361 (6407): 64 – 66. DOI:10.1038/361064a0.
- Sereno, P., & Novas, F. (1994). The Skull and Neck of the Basal Theropod *Herrerasaurus ischigualastensis*. *Journal of Vertebrate Paleontology*. 1994. 13.4: 451-76. Print. doi: 10.1080/02724634.1994.10011525.
- Sereno, P.C., 2005. TaxonSearch: Database for Suprageneric Taxa & Phylogenetic Definitions. <http://www.taxonsearch.org/>.
- Sereno, P., Martinez, R., & Alcober, O. (2013). Osteology of *Eoraptor lunensis* (Dinosauria, Sauropodomorpha). Basal sauropodomorphs and the vertebrate fossil record of the Ischigualasto Formation (Late Triassic: Carnian-Norian) of Argentina. *Journal of Vertebrate Paleontology Memoir*. 2013. 12: 83 – 179.  
DOI:10.1080/02724634.2013.820113

- Simmons, D. (1965). The non-therapsid reptiles of the Lufeng Basin, Yunnan, China. 1965. *Fieldiana: Geology* 15: 1 – 93.
- Smith, N., Makovicky, P., Hammer, W., & Currie, P. (2007). Osteology of *Cryolophosaurus ellioti* (Dinosauria: Theropoda) from the Early Jurassic of Antarctica and implications for early theropod evolution. *Zoological Journal of the Linnean Society*. 2007. 151(2): 377-421. DOI: 10.1111/j.1096-3642.2007.00325.x.
- Spiekman, S., Ezcurra, M., Butler, R., Fraser, N., & Maidment, S. (2021). *Pendraig milnerae*, a new small-sized coelophysoid theropod from the Late Jurassic of Wales. *Royal Society Open Science*. 8(10). doi: 10.1098/rsos.210915.
- Spiekman, S. (2023). A revision and histological investigation of *Saltoposuchus connectens* (Archosauria: Crocodylomorpha) from the Norian (Late Triassic) of south-western Germany. *Zoological Journal of the Linnean Society*. 199: 354 – 391. DOI: 10.1093/zoolinnea/zlad035.
- Sues, H., Shubin, N., and Olsen P. (1994). A new sphenodontian (Lepidosauria: Rhynchocephalia) from the Southern Hemisphere. *Canada Journal of Vertebrate Paleontology*. 14: 327 – 340.
- Sues, H., Nesbitt, S., Berman, D., & Henrici, A. (2011). A late-surviving basal theropod dinosaur from the latest Triassic of North America. *Proceedings of the Royal Society B: Biological Sciences*. 278(1723): 3459-3464. DOI: 10.1098/rspb.2011.0410.
- Sulej, T., Niedźwiedzki, G., & Bronowicz, R. (2012). A new Late Triassic vertebrate fauna from Poland with turtles, aetosaurs, and coelophysoid dinosaurs. *Journal of*

Vertebrate Paleontology. 32(5): 1033-1041. doi:

10.1080/02724634.2012.694384.Talbot,

Tykoski, R. (2005). Anatomy, ontogeny, and phylogeny of coelophysoid theropods (Unpublished doctor's thesis). University of Texas at Austin. Retrieved from <http://hdl.handle.net/2152/3992>.

von Huene, F. (1906). Über die Dinosaurier der aussereuropäischen Trias. Geologische und Paläontologische Abhandlungen. 1906. 8 (2): 97 – 156.

Von Huene, F. (1932). Die fossile Reptil-Ordnung Saurischia, ihre Entwicklung und Geschichte. Monographien zur Geologie und Paläontologie. 1 (4): 361

Wang, Y., You, H. & Wang, T. (2017). A new basal sauropodiform dinosaur from the Lower Jurassic of Yunnan Province, China. Scientific Report. 7: 41881. Doi: 10.1038/srep41881.

Wang, L., Clark, J., Li, H., Ruebenstahl, A., Bi, S. (2025). A new specimen of the early branching crocodyliform *Platyognathus hsui* extends the record of gobiosuchids back 67 million years, Zoological Journal of the Linnean Society, Volume 204, Issue 2, June 2025, zlaf032. doi: 10.1093/zoolinnean/zlaf032.

Welles, S. *Dilophosaurus wetherilli* (Dinosauria, Theropoda) osteology and comparisons. (1984). *Palaeontographica Abteilung A*. 185 (4 – 6): 85 – 180.

Wu, X. (1994). “Late Triassic-Early Jurassic sphenodontians from China and the phylogeny of the Sphenodontia.” In Fraser, N., and Sues, H. In the Shadow of the Dinosaurs: Early Mesozoic Tetrapods. Cambridge: Cambridge University Press. 38 – 69.

Wu, X., and Sues, H. (1996). Reassessment of *Platyognathus hsui* Young, 1944

(Archosauria: Crocodyliformes) from the Lower Lufeng Formation (Lower Jurassic) of Yunnan, China. *Journal of Vertebrate Paleontology*. 16:42–8. doi: 10.1080/02724634.1996.10011282.

Xu, X., You, H., & Mo, J. (2021). Saurichian Dinosaurs, *Palaeovertebrata Sinica* (Vol. II, No. 10). Beijing: Science Press. ISBN 978-7-03-070975-2.

You, H., Azuma, Y., Wang, T., Wang, Y., & Dong, Z. (2014). The first well-preserved Coelophysoid theropod dinosaur from Asia. *Zootaxa*. 3873(3), 233. doi: 10.11646/zootaxa.3873.3.3.

Young, C.-C. (1940). Preliminary note on the Mesozoic mammals of Lufeng, Yunnan, China. *Bulletin of the Geological Society of China* 20: 93–111.

Young, C.-C. (1941). A complete osteology of *Lufengosaurus hueni* Young (gen. et sp. nov.) from Lufeng, Yunnan, China. *Palaeontologica Sinica, Series C* 7, 1–53.

Young, C.-C. (1942). *Yunnanosaurus huangi* Young (gen. et sp. nov.), a new Prosauropoda from the Red Beds at Lufeng, Yunnan. *Bulletin of the Geological Society of China* 22(1–2), 63–104.

Young, C.-C. (1944). On a supposed new pseudosuchian from Upper Triassic saurischian-bearing beds of Lufeng Yunnan, China. *American Museum Novitates*. 1246: 1–4.

Young, C.-C. (1947a). Mammal-like reptiles from Lufeng, Yunnan, China. *Proceedings of the Zoological Society of London* 117: 537–597.

Young, C.-C. (1947b). On *Lufengosaurus magnus* Young (sp. nov.) and additional finds of *Lufengosaurus huenei* Young. *Palaeontologica Sinica, Series C* 12, 1–53.

Young, C.-C. (1948). On two new Saurischians from Lufeng, Yunnan. *Bulletin of the*

Geological Society of China. 28.1-2 (1948): 75-90. Wiley Online Library.

Young, C.-C. (1951). The Lufeng Saurischian Fauna in China. *Palaeontologia Sinica*, Series C 13, 1–94.

Young, C.-C. (1978). New material of *Eozostrodon*. *Vertebrata Palasiatica* 16: 1-3, [Original text in Chinese]

Young, C.-C. (1982). “A primitive fossil species of crocodylomorph from Lufeng, Yunnan.” in Collection of C.-C. Young. Beijing: Science Press. 26-28. [Original text in Chinese]

Zahner, M., & Brinkmann, W. (2019). A Triassic averostran-line theropod from Switzerland and the early evolution of dinosaurs. *Nature Ecology & Evolution*. 2019. DOI: 10.1038/s41559-019-0941-z.

Zhang, Q., You, H., Wang, T., and Chatterjee S. (2018). A new sauropodiform dinosaur with a 'sauropodan' skull from the Lower Jurassic Lufeng Formation of Yunnan Province, China. *Scientific Report*. Sep 7;8(1):13464. doi: 10.1038/s41598-018-31874-9.

Zhang, Q., Wang, T., Yang, Z., You, H. (2020). Redescription of the cranium of *Jingshanosaurus xinwaensis* (Dinosauria: Sauropodomorpha) from the Lower Jurassic Lufeng Formation of Yunnan Province, China. *Anat. Rec.* 303, 759–771. doi: 10.1002/ar.24113(2020).

Zhang, Q., Jia, L., Wang, T., Zhang, Y., and You H. (2024). The largest sauropodomorph skull from the Lower Jurassic, Lufeng Formation of China. *PeerJ* 12:e18629 DOI 10.7717/peerj.18629

Zhang, Y., and Yang, Z. (1985). *Jingshanosaurus* – a new species of prosauropods

from Lufeng basin sediments of China. Kunming: Yunnan Science and Technology Press. 1-100. [Original text in Chinese]

Zhang, Z., Wang, T., & You, H. (2023). A New Specimen of *Sinosaurus triassicus* (Dinosauria: Theropoda) from the Early Jurassic of Lufeng, Yunnan, China. Historical Biology. DOI: 10.1080/08912963.2023.2190760.

Zou, Y, Chen, L,

Wang, T., Wang G, Zhang W, Zhang, X, Wang. Z, Wu. X, and You, H.. (2025). A new metriacanthosaurid theropod dinosaur from the Middle Jurassic of Yunnan Province, China. PeerJ. 2025 Apr 2;13:e19218. doi: 10.7717/peerj.19218.

Zou, Y, Chen, L, Wang, T., Wang, G., Zhang, W., Zhang, X., Wang. Z., Wu. X., and You, H. (2025). A new metriacanthosaurid theropod dinosaur from the Middle

Jurassic of Yunnan Province, China. PeerJ. 2025 Apr 2;13:e19218. doi:

10.7717/peerj.19218. PMID: 40191750; PMCID: PMC11971988.